HHS Public Access

Author manuscript

Mol Microbiol. Author manuscript; available in PMC 2017 May 01.

Published in final edited form as:

Mol Microbiol. 2016 May ; 100(3): 510–526. doi:10.1111/mmi.13332.

Phosphate Starvation: a Novel Signal that Triggers ESX-5 Secretion in *Mycobacterium tuberculosis*

Sarah R. Elliott[1] and **Anna D. Tischler**[1,2,*]

[1]Department of Microbiology and Immunology, University of Minnesota Twin Cities, Minneapolis, MN 55455

[2]Center for Infectious Diseases and Microbiology Translational Research, University of Minnesota Twin Cities, Minneapolis, MN 55455

Summary

Mycobacterium tuberculosis uses the Type VII ESX secretion systems to transport proteins across its complex cell wall. ESX-5 has been implicated in *M. tuberculosis* virulence, but the regulatory mechanisms controlling ESX-5 secretion were unknown. Here we uncover a link between ESX-5 and the Pst/SenX3-RegX3 system that controls gene expression in response to phosphate availability. The DNA-binding response regulator RegX3 is normally activated by phosphate limitation. Deletion of *pstA1*, which encodes a Pst phosphate uptake system component, causes constitutive activation of RegX3. A Δ*pstA1* mutant exhibited RegX3-dependent over-expression of *esx-5* genes and hyper-secretion of the ESX-5 substrates EsxN and PPE41 when the bacteria were grown in phosphate-rich medium. In wild-type *M. tuberculosis,* phosphate limitation activated *esx-5* transcription and secretion of both EsxN and PPE41, and this response required RegX3. Electrophoretic mobility shift assays revealed that RegX3 binds directly to a promoter within the *esx-5* locus. Remarkably, phosphate limitation also induced secretion of EsxB, an effector of the virulence-associated ESX-1 secretion system, though this induction was RegX3 independent. Our work demonstrates that the Pst/SenX3-RegX3 system directly regulates ESX-5 secretion at the transcriptional level in response to phosphate availability and defines phosphate limitation as an environmental signal that activates ESX-5 secretion.

Keywords

Type VII secretion; ESX secretion; Pst phosphate uptake system; SenX3; RegX3; ESX-1

Introduction

Pathogenic bacteria often use specialized protein secretion systems to promote colonization, replication and survival within the host, and precise regulation of these virulence factors is critical to the success of the organism. All bacteria rely on the general housekeeping Sec secretion system, and many also maintain Tat export pathways to facilitate the transport of

*Contact: Anna D. Tischler, PhD. tischler@umn.edu Phone: 612-624-9685 Fax: 612-626-0623.

The authors have no conflicts of interest to declare.

proteins vital for cellular processes (Ligon *et al.*, 2012). *Mycobacterium tuberculosis*, a facultative intracellular pathogen and etiologic agent of the pulmonary infection tuberculosis, also possesses five ESX Type VII secretion systems designated ESX-1 through ESX-5. Each ESX system is comprised of the core secretion machinery components EccBm, EccC, EccD, and MycP (Stoop *et al.*, 2012). EccB is a transmembrane protein, EccC is an ATPase predicted to energize protein translocation, and MycP is a membrane-tethered protease that may play a role in substrate processing. EccD is also a transmembrane protein, which is predicted to form the inner membrane channel through which ESX substrates are secreted (Houben *et al.*, 2014). Esx proteins, the canonical substrates of the ESX systems, are ~100 amino acids in length and are usually encoded in pairs and secreted as heterodimers (Houben *et al.*, 2014). ESX systems also secrete two families of proteins unique to mycobacteria that are named PE and PPE proteins based on highly conserved N-terminal domains containing either proline-glutamic acid (PE) or proline-proline-glutamic acid (PPE) sequence motifs (Cole *et al.*, 1998). These proteins are also thought to be secreted as heterodimers, consisting of one PE and one PPE protein (Ekiert & Cox, 2014). The PE and PPE heterodimer requires interaction with its cognate EspG chaperone to be directed to the proper ESX secretion machinery for transport (Daleke *et al.*, 2012, Korotkova *et al.*, 2014, Ekiert & Cox, 2014). Though the function of most PE and PPE proteins remains unknown, several have recently been implicated in virulence and persistence (Sampson, 2011).

ESX-5 is the most recently evolved of the ESX secretion systems (Gey van Pittius *et al.*, 2001). While the exact function of ESX-5 is unknown, this system is found only in the slow-growing pathogenic mycobacteria, including *M. tuberculosis*, and increasing evidence supports a role for ESX-5 in virulence. ESX-5 secretion activates the inflammasome and IL-1β secretion, and induces necrotic cell death, thus promoting bacterial survival (Abdallah *et al.*, 2011). *M. tuberculosis* requires $EccD_5$, the putative ESX-5 transmembrane channel, for full virulence as disruption of *eccD*$_5$ causes a replication defect within murine macrophages and attenuation in severe combined immune-deficient (SCID) mice (Bottai *et al.*, 2012). Immune responses to certain PE and PPE epitopes are undetectable when *eccD*$_5$ is deleted, suggesting that these PE and PPE proteins are transported through ESX-5, and that ESX-5 actively secretes these proteins during infection (Sayes *et al.*, 2012). The *esx-5* locus encodes several PE and PPE proteins and the Esx protein EsxN. The *esxM* gene adjacent to *esxN* contains a frameshift mutation predicted to truncate EsxM, but there are four homologous *esxM/esxN* gene pairs outside of the *esx-5* locus, and it is probable that one of these alternative EsxM-like proteins pairs with EsxN (Houben *et al.*, 2014, Bottai *et al.*, 2012). The ESX-5 system secretes EsxN and the PE25/PPE41 heterodimer (Bottai *et al.*, 2012), but the mechanism(s) by which ESX-5 substrate secretion is regulated are currently unknown.

Mechanisms regulating activity of the related mycobacterial ESX-3 secretion system have been well characterized. ESX-3 is negatively regulated by the repressors IdeR and Zur in response to high levels of iron and/or zinc, respectively (Rodriguez *et al.*, 2002, Maciag *et al.*, 2007). These observations provided a clue to the function of ESX-3, which is involved in the import of iron, and possibly zinc (Siegrist *et al.*, 2009, Serafini *et al.*, 2009). Discovering factors that regulate ESX-5 activity may similarly provide insight into its function.

We previously demonstrated that the *M. tuberculosis* Pst/SenX3-RegX3 system controls gene expression in response to extracellular phosphate availability (Tischler *et al.*, 2013). The Pst (phosphate specific transport) system is an ABC type transporter that imports inorganic phosphate (P_i) across the cytoplasmic membrane using energy from ATP hydrolysis. In some bacterial species, in addition to its role in P_i uptake, the Pst system also plays a role in gene regulation through an interaction with a two-component signal transduction system (Lamarche *et al.*, 2008). The two-component system SenX3-RegX3, comprised of a membrane bound sensor histidine kinase and DNA binding response regulator, respectively, is activated during P_i limitation, and genes involved in P_i scavenging are part of its regulon (Tischler *et al.*, 2013). Genetic evidence suggests that the Pst system inhibits activation of SenX3-RegX3 when P_i is abundant. Deletion of *pstA1,* which encodes a transmembrane component of the Pst system, causes loss of this negative regulation of SenX3-RegX3, resulting in constitutive activation of RegX3, regardless of extracellular P_i levels (Tischler *et al.*, 2013). The SenX3-RegX3 two-component system is required for *M. tuberculosis* virulence (Parish *et al.*, 2003, Tischler *et al.*, 2013), likely because the bacteria must be able to activate the RegX3 regulon in response to P_i limitation encountered during infection to survive. The regulatory function of PstA1 is also required for *M. tuberculosis* virulence, which suggests that inappropriate constitutive activation of RegX3 and expression of its regulon is also detrimental to survival of the bacterium (Tischler *et al.*, 2013).

Transcriptional profiling experiments identified many genes that were differentially expressed by the Δ*pstA1* mutant compared to wild-type *M. tuberculosis* during growth in P_i-rich conditions. Genes in the *esx-5* locus were over-expressed by the Δ*pstA1* mutant, revealing a potential link between the P_i starvation responsive Pst/SenX3-RegX3 system and ESX-5 activity. Here we demonstrate that ESX-5 protein secretion is activated in response to P_i limitation. Regulation of ESX-5 activity is mediated by the Pst/SenX3-RegX3 system at the level of transcription of a subset of genes that are encoded in the *esx-5* locus. Further, we demonstrate that secretion of the ESX-1 substrate EsxB is also stimulated in response to P_i limitation, though this regulation is independent of the Pst/SenX3-RegX3 system. Our results have provided an important clue towards understanding the function of the ESX-5 secretion system and relevant environmental signals that may stimulate ESX secretion during infection.

Results

The ΔpstA1 mutant over-expresses esx-5 genes in a RegX3-dependent manner

Previously, we conducted microarray experiments to examine gene expression in a Δ*pstA1* mutant grown in P_i-rich medium (Tischler *et al.*, 2013). Of the 66 genes that were differentially expressed by Δ*pstA1* bacteria relative to the wild-type (WT) Erdman strain, several were located within the *esx-5* locus (Fig. 1A). Some *esx-5* genes were significantly over-expressed by the Δ*pstA1* mutant, including *ppe25, pe18, ppe27,* and *esxM* (relative fold change: 9.7, 3.6, 6.8, and 1.6, respectively) (Tischler *et al.*, 2013). Other genes in the *esx-5* locus were also over-expressed, though the difference in expression level for these genes did not achieve statistical significance: *pe19, espG*$_5$*, eccD*$_5$*, esxN* and *mycP*$_5$ (relative fold change: 4.09, 2.91, 1.7, 1.5, and 1.56, respectively) (Tischler *et al.*, 2013). To confirm these

results and test whether additional genes in the *esx-5* locus were similarly over-expressed, we conducted quantitative reverse transcription PCR (qRT-PCR) experiments. Consistent with the transcriptional profiling, the *esxM* and *esxN* transcripts were over-expressed approximately 2-fold by the Δ*pstA1* mutant compared to the WT control (Fig. 1B). Additionally, $espG_5$, $eccD_5$, and $mycP_5$ transcripts were significantly over-expressed by the Δ*pstA1* mutant strain relative to WT (fold change = 4, 2.7, and 2; $P = 0.001$, 0.0025, and 0.046, respectively). In contrast, the $eccB_5$ transcript, which is located in a separate operon on the 5' end of the *esx-5* locus (Fig. 1A), was not significantly over-expressed by the Δ*pstA1* mutant (Fig. 1B). These data indicate that only the genes located at the 3' end of the *esx-5* locus are aberrantly expressed by the Δ*pstA1* mutant.

We previously demonstrated that aberrant gene expression in the Δ*pstA1* mutant is dependent on the RegX3 DNA-binding response regulator (Tischler *et al.*, 2013). To determine if RegX3 is responsible for over-expression of *esx-5* genes by the Δ*pstA1* mutant, we examined *esx-5* transcript levels in Δ*regX3,* Δ*pstA1*Δ*regX3* and the respective pND*regX3* complemented strains. Expression of the *esxM, esxN,* $espG_5$, $eccD_5$ and $mycP_5$ transcripts was restored to the WT level in Δ*pstA1*Δ*regX3* bacteria (Fig. 1B). These changes in *esx-5* expression were attributable to deletion of *regX3* because complementation with *regX3* expressed *in trans* (Δ*pstA1*Δ*regX3* pND*regX3*) restored significant over-expression of the $espG_5$, $eccD_5$, and $mycP_5$ transcripts compared to WT ($P = 0.04$, 0.01, and 0.02, respectively) (Fig. 1B). These data suggest that *esx-5* genes are over-expressed by Δ*pstA1* bacteria due to constitutive activation of RegX3.

Hyper-secretion of ESX-5 substrates by the ΔpstA1 mutant requires RegX3

To determine if over-expression of *esx-5* genes by the Δ*pstA1* mutant affects activity of the ESX-5 secretion system, we performed Western blots to monitor the secretion of two known ESX-5 substrates, EsxN and PPE41 (Bottai *et al.*, 2012). EsxN was undetectable in the cell lysate fractions, but was hyper-secreted by the Δ*pstA1* mutant compared to WT (Fig. 2). Since EsxN secretion was undetectable in the WT control, we quantified the increase in EsxN secretion by performing Western blots on decreasing amounts of the Δ*pstA1* mutant culture filtrate. EsxN secretion became undetectable when 0.5 μg of total culture filtrate protein was loaded, suggesting at least 8-fold induction of EsxN secretion in the Δ*pstA1* mutant compared to WT (Fig. S1). This induction of EsxN secretion exceeded the roughly 2-fold increase in *esxN* transcription that we detected in the Δ*pstA1* mutant (Fig. 1B). PPE41 was detectable in the cell lysate fraction only upon prolonged exposure of the blot, but was present in higher abundance in the Δ*pstA1* mutant compared to WT (Fig. 2). We also observed approximately 4-fold hyper-secretion of PPE41 by the Δ*pstA1* mutant compared to WT (Fig. 2 and Fig. S1), though we detected no significant difference in *ppe41* transcript abundance (Fig. 1B). ModD, a protein secreted by the general Sec secretion system, was detected in equivalent amounts in the culture filtrate fractions of WT and Δ*pstA1* bacteria, confirming equivalent protein loading, and demonstrating that the Δ*pstA1* mutation does not globally affect other secretion pathways (Fig. 2). We routinely detect ModD as a doublet in our experiments, which is consistent with previously observed glycosylation of this protein (Dobos *et al.*, 1995). GroEL2, a cell-associated protein, was undetectable in the culture filtrate, verifying there was no cell lysis (Fig. 2). These data

indicate potential post-transcriptional regulation of both EsxN and PPE41 secretion, as in each case the fold change in protein secretion was substantially greater than the change in transcript abundance.

To determine whether the Δ*pstA1* mutation alters expression of the ESX-5 secretion system itself, we examined production of the ESX-5 conserved components $EspG_5$ and $EccB_5$. PPE41 requires an interaction with its cognate chaperone $EspG_5$ for secretion via the ESX-5 system (Daleke *et al.*, 2012). We observed 4-fold overproduction of $EspG_5$ in the cell lysate fraction of Δ*pstA1* bacteria (Fig. 2), which correlated well with the 4-fold over-expression of the *espG*$_5$ transcript (Fig. 1B). $EccB_5$ is a core component of the ESX-5 secretion apparatus (Houben *et al.*, 2012b). We observed 2-fold over-production of $EccB_5$ in the Δ*pstA1* mutant compared to the WT strain (Fig. 2 and Fig. S1), despite no evidence for transcriptional regulation of the *eccB*$_5$ gene (Fig. 1B). GroEL2, the cell lysate loading control, was detected in equal amounts in WT and Δ*pstA1* bacteria confirming equivalent protein loading (Fig. 2). These data indicate post-transcriptional regulation of $EccB_5$ protein production or stability. Increased production of the ESX-5 secretion machinery and the $EspG_5$ chaperone may contribute to the enhanced secretion of EsxN and PPE41, respectively, that we observe in the Δ*pstA1* mutant.

To determine if the increase in ESX-5 protein production and secretion by the Δ*pstA1* mutant requires RegX3, Western blots were performed on proteins isolated from the Δ*regX3*, Δ*pstA1*Δ*regX3* and the respective pND*regX3* complemented strains. EsxN and PPE41 were not hyper-secreted by the Δ*pstA1*Δ*regX3* mutant (Fig. 2). The cell-associated proteins $EspG_5$ and $EccB_5$ were also produced at WT levels by the Δ*pstA1*Δ*regX3* strain (Fig. 2). Complementation of the *regX3* deletion *in trans* (Δ*pstA1*Δ*regX3* pND*regX3*) restored ESX-5 protein production and secretion to amounts comparable to those observed in the Δ*pstA1* mutant (Fig. 2). The GroEL2 and ModD controls confirmed equivalent protein loading among the WT, Δ*pstA1*Δ*regX3,* and Δ*pstA1*Δ*regX3* pND*regX3* strains and verified that cell lysis did not contribute to proteins present in the culture filtrate (Fig. 2). These results indicate that increased production of ESX-5 secretion system components and hyper-secretion of ESX-5 substrates by the Δ*pstA1* mutant require the DNA-binding response regulator RegX3.

esx-5 gene expression is induced by phosphate limitation

Because the SenX3-RegX3 two-component system is activated by P_i limitation (Tischler *et al.*, 2013), we predicted that *esx-5* genes would be induced in a RegX3-dependent manner by P_i-limiting conditions. To test this prediction, we grew WT, Δ*regX3* and Δ*regX3* pND*regX3* strains in P_i-free 7H9 medium, and monitored gene expression over time by qRT-PCR. The *esxN, espG*$_5$, and *eccD*$_5$ transcripts were all significantly induced 2.5- to 4-fold in WT bacteria after 24 hours of P_i limitation (*P*-values: 0.001, 0.03, and 0.008, respectively), and abundance of these transcripts remained significantly elevated for the duration of the experiment (Fig. 3A-C). There was no induction of either *eccD*$_5$ or *espG*$_5$ transcription in the Δ*regX3* mutant in response to P_i limitation (Fig. 3B and C). The Δ*regX3* mutant did exhibit a 2-fold increase in *esxN* transcription at 24 and 48 hours and this induction was statistically significant ($P = 0.04$ and 0.003, respectively), but was not sustained at the 72

and 96 hour time points (Fig. 3A). In addition, the level of *esxN* transcript in the Δ*regX3* mutant was significantly lower than the WT control at 24 hours ($P = 0.025$) and all subsequent time points (Fig. 3A). Complementation of the Δ*regX3* mutation *in trans* restored rapid induction and continuous elevated expression of the *esxN, espG*$_5$, and *eccD*$_5$ genes (Fig. 3A-C). These data demonstrate that activation of *esx-5* gene expression in response to P_i limitation requires *regX3.*

Because *eccB*$_5$ was not significantly over-expressed by the Δ*pstA1* mutant in P_i-rich medium (Fig. 1B, $P = 0.24$), we did not expect this gene to be induced by P_i limitation. We observed a modest 2.2-fold increase in abundance of the *eccB*$_5$ transcript in WT bacteria that was statistically significant ($P = 0.014$), but occurred only after 96 hours of P_i limitation (Fig. 3D). Induction of *eccB*$_5$ transcript was not observed in the Δ*regX3* mutant, but this phenotype could not be complemented *in trans* (Fig. 3D). These data suggest that RegX3-dependent regulation of *esx-5* transcription is restricted to those genes located at the 3' end of the *esx-5* locus. Finally, though it is located outside the *esx-5* locus, we examined transcription of *ppe41*. The level of *ppe41* transcript increased approximately 2-fold in WT bacteria during P_i limitation, but this induction was not statistically significant (Fig. 3E). However, maintenance of this high level of *ppe41* transcription required RegX3 (Fig. 3E). The level of *ppe41* transcript was reduced 4-fold in the Δ*regX3* mutant within 48 hours of P_i limitation, the decrease was statistically significant ($P = 0.0017$) and this phenotype could be complemented *in trans* (Fig. 3E). These data indicate that RegX3 contributes to maintenance of *ppe41* transcription during P_i limitation, whether directly or indirectly.

Secretion of ESX-5 and ESX-1 substrates is induced by phosphate limitation

Since expression of some *esx-5* genes was induced by P_i limitation, we predicted that ESX-5 protein secretion would also be induced by this growth condition. Our initial attempts to monitor ESX-5 protein secretion in P_i-free medium were unsuccessful, likely due to insufficient bacterial growth (data not shown). We therefore conducted experiments to identify a P_i concentration that would be sufficient to sustain growth and yet restrictive enough to activate the P_i starvation-responsive Pst/SenX3-RegX3 system. The analogous two-component system in *E. coli*, PhoRB, is activated by P_i concentrations below 4 μM (Lamarche *et al.*, 2008). To ensure minimal carryover of residual P_i into the cultures used to test protein secretion, we pre-grew the bacteria in Sauton's medium containing only 250 μM P_i, a concentration we determined is sufficient to support a rate of bacterial growth similar to that observed in complete Sauton's medium (data not shown). We then monitored ESX-5 secretion by WT *M. tuberculosis* across a 100-fold range of P_i concentrations in Sauton's medium, including a P_i concentration (2.5 μM) predicted to activate RegX3 and therefore induce ESX-5 secretion.

Consistent with the results of our qRT-PCR experiments, in P_i-limited medium we observed a 9-fold increase in production of $EspG_5$ (Fig. 4). Indeed, production of $EspG_5$ steadily increases as the P_i concentration decreases, with the highest protein production observed at 2.5 μM P_i (Fig. 4). Similarly, EsxN secretion is induced in P_i-limited medium and is the most evident when bacteria are cultured with 2.5 μM P_i (Fig. 4). Although we did not observe significant changes in transcription of *eccB*$_5$ or *ppe41* in WT bacteria grown in P_i-

limited conditions, $EccB_5$ protein production and PPE41 secretion were also induced in response to P_i limitation (Fig. 4). We observed an 8-fold increase in production of $EccB_5$ and induction of PPE41 secretion at 2.5 μM P_i (Fig. 4). These data demonstrate that ESX-5 secretion is activated by P_i limitation. They also suggest that $EccB_5$ production or stability and PPE41 secretion are post-transcriptionally regulated during P_i limitation.

In these experiments, we observed a marked decline in secretion of ModD, our Sec-secreted control, in P_i-limited growth conditions (Fig. 4). At 2.5 μM P_i, ModD secretion was decreased approximately 4-fold. The decrease in ModD secretion during P_i limitation is not completely explained by a modest and statistically insignificant 2-fold decrease in *modD* transcript abundance (Fig. 3F). To determine whether this effect of P_i limitation on ModD secretion was generalizable to other Sec-secreted proteins, we examined secretion of the antigen 85 complex (Ag85). Secretion of Ag85 was also reduced roughly 3-fold at 2.5 μM P_i, with a concomitant accumulation of Ag85 in the cell lysate fraction (Fig. 4). These data suggest that P_i limitation also causes decreased activity of the general Sec secretion system.

To determine if P_i limitation globally affects *M. tuberculosis* protein secretion, we examined secretion of EsxB (CFP-10), an Esx protein secreted via the ESX-1 system that has a well-established role in *M. tuberculosis* virulence (Hsu *et al.*, 2003, Stanley *et al.*, 2003, Guinn *et al.*, 2004, de Jonge *et al.*, 2007, Houben *et al.*, 2012a, Manzanillo *et al.*, 2012). We observed less EsxB in the cell lysate fraction and a concurrent increase in EsxB in the culture filtrate fraction at lower P_i concentrations (Fig. 4). Although EsxB secretion was undetectable in 4 μg of secreted protein from P_i-rich control cultures, when 8 μg of secreted protein were loaded we could readily detect EsxB in all samples. We observed a roughly 7-fold increase in EsxB secretion at 2.5 μM P_i (Fig. 4). The change in distribution of EsxB cannot be explained by differences in cell lysate protein loading or contamination of the culture filtrate fraction by cell lysis, based on the GroEL2 control (Fig. 4). To determine whether activity of the ESX-1 system is generally increased during P_i limitation, we examined secretion of a second ESX-1 substrate, EspB (McLaughlin *et al.*, 2007). We detected EspB secretion at all P_i concentrations examined, with an approximately 2-fold increase in EspB secretion at 2.5 μM P_i in the experiment shown (Fig. 4), though this result was not reproducible. These data indicate that secretion or release of the ESX-1 substrate EsxB, rather than activity of the ESX-1 system, is increased during P_i limitation.

To determine if increased EsxB secretion in P_i limited growth conditions was due to a change in *esxB* expression, we monitored *esxB* transcript abundance. Although there was a nearly 2-fold increase in *esxB* expression during P_i limitation in WT bacteria, this induction was not statistically significant (Fig. 3G). We also examined expression of *espA*, since secretion of EsxB is dependent on expression of the *espACD* operon and several transcriptional regulators are known to act at this locus (Raghavan *et al.*, 2008, Pang *et al.*, 2013). The *espA* transcript increased approximately 2.5-fold in abundance after 96 hours of P_i limitation, but this change in *espA* expression was not statistically significant (Fig. 3H). These results suggest that increased secretion of the ESX-1 substrate EsxB secretion in response to P_i limitation occurs at the post-transcriptional level.

Phosphate limitation, not potassium limitation, causes increased secretion of ESX-1 and ESX-5 substrates

In the experiments we conducted to determine if P_i limitation induces ESX-5 protein secretion, we used monopotassium phosphate (KH_2PO_4) as a P_i source. By limiting the source of P_i, we also inadvertently limited the only source of potassium (K^+) in the medium. K^+ is critical for many bacterial processes, including maintaining an electrochemical gradient and regulating intracellular pH (Epstein, 2003). We tested whether the induction of ESX-5 and ESX-1 secretion was due to either K^+ or P_i limitation, or perhaps both. We grew WT *M. tuberculosis* in P_i and K^+ limiting conditions identical to those used in our previous experiments, and in conditions where only P_i or K^+ was the limiting nutrient. Consistent with our previous experiments, both EsxN and EsxB were hyper-secreted in medium that was limiting for both P_i and K^+ (Fig. 5). We observed similar hyper-secretion of both EsxN and EsxB when WT *M. tuberculosis* was grown in medium that was only limiting for P_i (Fig. 5). In contrast, neither EsxN nor EsxB was hyper-secreted in K^+-limited medium (Fig. 5). GroEL2 was undetectable in the culture filtrate fractions, confirming that the culture filtrates were not contaminated by cell lysis. ModD secretion was unaffected by K^+ limitation, but decreased in both cultures with limiting amounts of P_i (Fig. 5). These data indicate that P_i limitation is a relevant signal that induces secretion of EsxN and EsxB.

RegX3 is required for induction of ESX-5 secretion in phosphate limiting conditions

Secretion of the ESX-5 substrates EsxN and PPE41 and the ESX-1 substrate EsxB is induced under P_i-limiting conditions. To determine if this induction is dependent on the response regulator RegX3, we grew WT, Δ*regX3* and Δ*regX3* pND*regX3* strains in medium containing either 4 mM P_i (control) or 2.5 μM P_i. We chose to use the lowest P_i concentration that was tested in our preliminary experiments because we observed the highest levels of EsxN, PPE41 and EsxB protein secretion at this concentration. Hyper-secretion of the ESX-5 substrates EsxN and PPE41 in P_i-limiting conditions was dependent on RegX3. Unlike the WT or Δ*regX3* pND*regX3* complemented strains, the Δ*regX3* strain did not induce EsxN or PPE41 secretion under P_i-limiting conditions (Fig. 6). RegX3 was also required for increased $EspG_5$ and $EccB_5$ protein production under P_i-limiting conditions (Fig. 6). These data suggest that RegX3-dependent transcriptional activation of a subset of *esx*-5 genes during P_i limitation leads to increased production of ESX-5 secretion system components and activation of ESX-5 substrate secretion.

We also examined secretion of the ESX-1 substrates EsxB and EspB. EsxB secretion was induced in the WT strain under P_i-limiting conditions, but this secretion was independent of RegX3, since we still observed hyper-secretion of EsxB in the Δ*regX3* mutant (Fig. 6). Secretion of a second ESX-1 substrate, EspB, was unchanged by P_i limitation in these experiments (Fig. 6). These data suggest the existence of an alternative P_i-starvation sensing mechanism that regulates secretion of the ESX-1 substrate EsxB.

RegX3 directly regulates esx-5 transcription by binding a promoter upstream of pe19

Our results indicate that RegX3 controls ESX-5 secretion at the transcriptional level, though the data do not differentiate between direct or indirect regulation. To determine if RegX3 directly regulates *esx-5* transcription, we sought to identify RegX3 binding sites within the

esx-5 locus. We previously observed that the *pe19* gene, which is located upstream of *esxN*, *espG*$_5$ and *eccD*$_5$ at the 3' end of the *esx-5* locus (Fig. 7A), is over-expressed by the Δ*pstA1* mutant and induced during P_i limitation in a RegX3-dependent manner (Ramakrishnan *et al.*, 2016). As part of our prior work, we also demonstrated that deletion of the *ppe27-pe19* locus, including the 426 bp intergenic region, caused a severe *in vitro* growth defect that could not be complemented *in trans* (Ramakrishnan *et al.*, 2016). These results suggested that the Δ*ppe27-pe19* mutation is polar on expression of the downstream *esx-5* genes. We therefore hypothesized that the 426 base pair intergenic region between *ppe27* and *pe19* contains a RegX3-dependent promoter that controls transcription of *esx-5* genes (Fig. 7A).

To test this hypothesis, we examined *esx-5* gene expression in strains harboring deletions within the *ppe27-pe19* locus that we previously constructed (Ramakrishnan *et al.*, 2016). Deletion of *ppe27-pe19* including the intergenic region (Δ*ppe27-pe19*) in the Δ*pstA1* background restored expression of *esxN*, *espG*$_5$, and *eccD*$_5$ to WT levels (Fig. 7B). In contrast, *esx-5* transcript levels remained elevated in the Δ*pstA1*Δ*ppe27* and Δ*pstA1*Δ*pe19* strains, which both retain an intact intergenic region (Fig. 7B). These data suggest that the *ppe27-pe19* intergenic region contains regulatory elements that are necessary for the RegX3-dependent over-expression of *esx-5* genes that we observed in the Δ*pstA1* mutant.

To narrow down the approximate location of RegX3-dependent transcription initiation, we performed qRT-PCR using primers spanning the *ppe27-pe19* intergenic region (Fig. 7A). The *pe19* transcript is over-expressed 4-fold in the Δ*pstA1* mutant compared to both the WT and Δ*pstA1*Δ*regX3* strains ($P = 0.02$ and 0.01, respectively, Fig. 7C). We predicted that amplicons within the intergenic region located 3' of the site of transcription initiation would exhibit a similar expression pattern in these three strains. We found that the Ig4 amplicon was overexpressed 4-fold in the Δ*pstA1* mutant compared to both the WT and Δ*pstA1*Δ*regX3* strains ($P = 0.03$ and 0.02, respectively, Fig. 7C). In contrast, neither the Ig1 nor Ig3 amplicons were significantly over-expressed by the Δ*pstA1* mutant (Fig. 7C). These data suggest that RegX3-dependent initiation of transcription likely occurs between the Ig3F and Ig4F primers.

To determine if transcripts initiating upstream of Ig4F can extend into the *esx-5* locus, we performed standard RT-PCR. Using primers Ig4F and esxNR3 (Fig. 7A), we detected the predicted 828 bp transcript in the WT, Δ*pstA1* and Δ*pstA1*Δ*regX3* strains grown in P_i-rich medium (Fig. 7D). Although the assay is not quantitative, we consistently observed increased intensity of the PCR product in the Δ*pstA1* mutant relative to the WT control that was RegX3-dependent (Fig. 7D). We also observed increased intensity of the Ig4F-esxNR3 PCR product in samples from the WT strain grown in P_i-limited conditions relative to the P_i-rich control (Fig. 7D). We were unable to amplify a PCR product from cDNA using the Ig3F and esxNR3 primers, providing further evidence that transcription is initiated between Ig3F and Ig4F (data not shown). Importantly, we did not detect PCR products in the no reverse transcriptase controls, indicating the RNA was not contaminated with genomic DNA (Fig. 7D). To establish whether full-length *esxN* and *espG*$_5$ are included in the operon initiating 5' of Ig4F, we performed similar RT-PCR experiments using the Ig4F and espG$_5$R1 primers (Fig. 7A). We detected a 1.8 kb PCR product, confirming that *pe19*, *esxN* and *espG*$_5$ are transcribed as an operon (Fig. 7D). Notably, we did not detect this transcript in RNA

extracted from the Δ*regX3* mutant grown in P_i-limiting conditions (Fig. 7D). We attempted to determine if this transcript extends into *eccD*$_5$ using reverse primers within the *eccD*$_5$ gene, but were not able to detect any PCR product (data not shown).

To determine if RegX3 binds directly to the *ppe27-pe19* intergenic region to promote transcription of *esx-5* genes, we purified recombinant His_6-RegX3 and performed electrophoretic mobility shift assays (EMSAs). Two probes were designed within the intergenic region to span the putative RegX3-dependent promoter (Fig. 7A). As a positive control, we generated a probe for a region 5' of *senX3*, to which RegX3 is known to bind (Himpens *et al.*, 2000). Using a range of His_6-RegX3 concentrations, we found that RegX3 bound to the *senX3* probe and Probe A with similar affinity (Fig. 7E). In contrast, RegX3 was unable to bind Probe B, even at the highest protein concentration tested (Fig. 7E). These data suggest that RegX3 binds directly to a sequence within the *ppe27-pe19* intergenic region located between positions −151 and −27 relative to the PE19 translational start site. To investigate the specificity of this binding, we performed EMSAs in the presence of competitors. An excess of specific unlabeled competitor resulted in a reversal of the mobility shift for both the *senX3* probe and Probe A (Fig. 7F). Addition of excess non-specific unlabeled competitor did not alter the observed mobility shift for either probe (Fig. 7F). These results suggest that the binding interaction between RegX3 and Probe A is DNA sequence specific. To demonstrate that RegX3, and not a contaminating protein, is responsible for the observed mobility shift, α-His_6 antibodies were added to the binding reactions. We observed a supershift for both probes (Fig. 7F), indicating the His_6-RegX3 protein specifically binds both the *senX3* promoter and the *ppe27-pe19* intergenic region. These data demonstrate that RegX3 directly controls *esx-5* transcription by binding to a promoter located upstream of *pe19*.

Discussion

While an intact ESX-5 secretion system is required for full virulence of *M. tuberculosis*, the environmental signal that induces ESX-5 activity was previously unknown. We demonstrate that ESX-5 protein production and secretion are induced during P_i limitation, a nutritional signal that may be encountered by *M. tuberculosis* during infection. Our data support a model in which activation of ESX-5 secretion during P_i limitation is mediated by the P_i starvation responsive Pst/SenX3-RegX3 system that directly regulates transcription of a subset of *esx-5* genes (Fig. 8).

The Pst phosphate uptake system regulates gene expression in response to P_i availability by interacting with the SenX3-RegX3 two-component system (Tischler *et al.*, 2013). In our model, when external P_i is abundant, the Pst system inhibits activation of SenX3-RegX3, *esx-5* genes are expressed at a basal level, and the ESX-5 system is in effect "off" (Fig. 8). However, when P_i is limiting, inhibition of SenX3-RegX3 is relieved, resulting in activation of *esx-5* transcription and switching ESX-5 secretion "on" (Fig. 8). We provide evidence that RegX3 directly activates transcription of *esx-5* genes in response to low P_i by binding to DNA upstream of *pe19*, leading to increased production of ESX-5 conserved components and increased secretion of the substrates EsxN and PPE41. Notably, deletion of *pstA1* prevents inhibition of SenX3-RegX3 by the Pst system in P_i-rich conditions, resulting in

constitutive activation of RegX3. In the Δ*pstA1* mutant, *esx-5* genes are constitutively expressed and ESX-5 is always “on”, leading to hyper-secretion of ESX-5 substrates, regardless of external P_i availability.

Our data indicate that RegX3 binds directly to the *ppe27*-pe19 intergenic region to promote *esx-5* transcription. Recent genome-wide transcriptional start site mapping has uncovered two start sites within this intergenic region at −38 and −133 relative to the PE19 translational start (Cortes *et al.*, 2013, Shell *et al.*, 2015). Our qRT-PCR data suggest there is a third transcriptional start site that is active in the Δ*pstA1* mutant and is RegX3-dependent. This putative RegX3-dependent transcriptional start site is located between the 5’ end of the Ig3F primer and the 5’ end of the Ig4F primer, at −90 and −46 relative to the PE19 translational start, respectively. It is likely that RegX3 binds upstream of this region to promote transcription. We analyzed the Probe A sequence (encompassing a region from −151 to −27), to which RegX3 can bind, for direct and inverted repeats. We found a 5 bp imperfect direct repeat sequence separated by 5 bp (GGTGCcaactGGTGA) located at -114 to -106 relative to the PE19 translational start site, within the region that we predict is likely to bind RegX3. Using similar analysis, we found a related repeat sequence (GGTGTgctttGGTGC) within the *senX3* probe. These direct repeat sequences may represent sites of RegX3 binding. Our future work will focus on determining the precise RegX3 binding site and mechanism of *esx-5* transcriptional regulation.

Although ESX-5 induction in response to P_i limitation occurs at the transcriptional level by RegX3-dependent activation of a subset of *esx-5* genes, our observations suggest post-transcriptional regulation of some ESX-5 conserved components and substrates. Though we observed over-production of $EccB_5$ during P_i limitation, the *eccB*$_5$ transcript was not induced by this growth condition, suggesting post-transcriptional regulation of $EccB_5$ translation or stability. $EccB_5$ is a member of the ESX-5 membrane complex, along with $EccC_5$, $EccD_5$, and $EccE_5$ (Houben *et al.*, 2012b). Over-production of $EccB_5$ in P_i-limited conditions may be due to enhanced stability of the protein mediated by increased production of other members of the membrane complex, including $EccD_5$, which is induced at the transcriptional level in these conditions. We also observed a greater increase in EsxN protein secretion compared to the change in *esxN* transcription. It is possible that additional EsxN is secreted due to enhanced production and activity of the ESX-5 core secretion machinery, both in the Δ*pstA1* mutant and during P_i limitation. Finally, we observed increased secretion of the ESX-5 substrate PPE41, though transcription of *ppe41* was not induced during P_i limitation. PPE41 is directed to the ESX-5 system for secretion by $EspG_5$, a protein chaperone that binds to PE and PPE proteins secreted by the ESX-5 system, including PPE41 (Daleke *et al.*, 2012, Korotkova *et al.*, 2014, Ekiert & Cox, 2014). Increased production of $EspG_5$ during P_i limitation may serve to stabilize PPE41, leading to the increased secretion we detected. Other PE and PPE protein pairs chaperoned by $EspG_5$ may also be hyper-secreted by ESX-5 during P_i limitation. Such post-transcriptional regulation of ESX-5 may allow the bacterium to undergo substantial changes in the ESX-5 secretome mediated by increased transcription of a small subset of genes that are required for stabilization of the system and its substrates.

While P_i limitation induces ESX-5 activity, this condition seems to result in decreased secretion via the general Sec protein secretion system. We detected reduced secretion of both ModD and the antigen 85 complex, which are Sec system substrates, during P_i limitation. The 4-fold decrease in ModD secretion that we observed is only partially explained by the 2-fold decrease in *modD* transcription under P_i-limiting conditions. In addition, we observed accumulation of the antigen 85 complex in the cell lysate fraction during P_i limitation, suggesting its secretion was prevented. Decreased protein secretion by the Sec system may reflect less available ATP to power Sec secretion. The ESX systems also require ATP for the transport of proteins (Houben *et al.*, 2014), and perhaps priority for protein secretion during P_i limitation goes to ESX-5. Alternatively, it is possible that there are simply less Sec secreted proteins in the culture filtrate as a fraction of the total amount of secreted proteins due to increased export of ESX-5 substrates and the ESX-1 substrate EsxB.

During our examination of the activating signal driving ESX-5 secretion, we discovered that P_i limitation also triggers secretion of the ESX-1 substrate EsxB (CFP-10). Induction of EsxB secretion is not dependent on RegX3, because enhanced EsxB secretion still occurs in a Δ*regX3* mutant. Since the Δ*regX3* mutant does not exhibit increased ESX-5 activity, hyper-secretion of EsxB is likely not dependent on the ESX-5 secretion system. Increased EsxB secretion in response to P_i limitation appears to occur at the post-transcriptional level, since transcription of *esxB* was not significantly induced during P_i starvation. We did observe a modest 2-fold increase in *espA* transcription during P_i starvation, which may contribute to increased secretion of EsxB, since EspA and EsxB exhibit co-dependent secretion (Fortune *et al.*, 2005). In contrast, secretion of the ESX-1 substrate EspB was unchanged during P_i limitation, suggesting that P_i limitation does not alter overall activity of ESX-1. It is possible that increased secretion of EsxB during P_i limitation reflects a change in kinetics of EsxB secretion or release of EsxB from a cell surface-associated location (Kennedy *et al.*, 2014) rather than a change in ESX-1 activity. The differences in secretion of the ESX-1 substrates EsxB and EspB during P_i limitation may also be caused by differences in their mechanisms of export, since EspB secretion is independent of both EsxB and EspA (McLaughlin *et al.*, 2007, Chen *et al.*, 2013).

Since the increased EsxB secretion in P_i-limiting conditions is not dependent on RegX3, our data suggest that an additional, as yet unknown, P_i sensing mechanism exists and is responsible for activating EsxB secretion. The ESX-1 transcriptional regulators that have been identified to date, including the nucleoid associated protein EspR and the two-component systems PhoPR and MprAB, have not been implicated in P_i sensing (Gonzalo-Asenio *et al.*, 2008, Raghavan *et al.*, 2008, Pang *et al.*, 2013, Zhang *et al.*, 2014). ESX-1 activity is also controlled by an ATP binding protein EspI, which negatively regulates secretion of the ESX-1 substrates EsxA, EsxB and EspB in response to low cellular ATP concentration (Zhang *et al.*, 2014). It is possible that downstream physiological changes the bacteria undergo during P_i limitation, perhaps including changes in ATP concentration, are the driving force behind EsxB secretion, as opposed to P_i availability being sensed directly. Hundreds of genes that are not part of the RegX3 regulon are differentially expressed in response to P_i limitation (Rifat *et al.*, 2009), and it is possible one of these factors is responsible for inducing EsxB secretion under these conditions. Regardless, we discovered

that P_i starvation is an environmental signal that triggers secretion of the ESX-1 substrate EsxB, though the precise mechanism by which this occurs will require further investigation.

P_i, an essential nutrient, is a component of many lipids, sugars, and nucleic acids, and is required for many cellular processes, including energy storage and signal transduction. *M. tuberculosis* is a facultative intracellular pathogen which may face conditions with low P_i availability *in vivo.* Within the lung, the bacterium resides inside the phagosomal compartment of infected macrophages, where the environment is harsh and predicted to be nutrient poor (Russell *et al.*, 2010). It is possible that P_i is a limiting nutrient within phagosomes, but the P_i concentration in mycobacterial phagosomes has not been measured with any certainty. While the amount of elemental phosphorus within the phagosomes of cultured murine macrophages decreased approximately 1.5-fold after 24 hours of infection with either *M. tuberculosis* or the related virulent species *M. avium* (Wagner *et al.*, 2005, Wagner *et al.*, 2006), there was no available calibration control to allow determination of the phosphorus concentration. It is therefore unclear if this change in phosphorus availability within the macrophage phagosome would be predicted to starve *M. tuberculosis* for P_i. During the chronic phase of infection, *M. tuberculosis* persists within foamy macrophages inside granulomas, the signature feature of a tuberculosis infection. Foamy macrophages accumulate lipid droplets, which primarily contain cholesterol (Russell *et al.*, 2009), and *M. tuberculosis* is able to survive by utilizing host lipids found within these lipid bodies (Peyron *et al.*, 2008). Cholesterol does not contain any phosphorus so foamy macrophages within the granuloma are another niche encountered by *M. tuberculosis* that may have a limiting concentration of P_i. It will be important to determine when and where *M. tuberculosis* encounters P_i limitation during the course of infection to uncover when ESX-5 is active and when its activity is critical for virulence.

We have discovered that P_i starvation is an environmental signal that activates ESX-5 secretion, and the Pst/SenX3-RegX3 system is required for this response. The Pst/SenX3-RegX3 system plays an important role during *M. tuberculosis* infection, considering that both Δ*pstA1* and Δ*regX3* mutants are attenuated in the murine aerosol infection model (Tischler *et al.*, 2013). Attenuation of these mutants may be explained by inappropriate regulation of ESX-5 secretion. The Δ*pstA1* mutant constitutively hyper-secretes ESX-5 substrates, some of which are known to be highly antigenic (Sayes *et al.*, 2012). We suspect that the Δ*pstA1* mutant is attenuated *in vivo* due to enhanced susceptibility to host immune responses driven by inappropriate secretion of ESX-5 antigens. Conversely, the Δ*regX3* mutant may be attenuated due to an inability to activate ESX-5 secretion in response to P_i limitation. We liken these dichotomous interpretations to a Goldilocks effect, since either constitutive ESX-5 hyper-secretion or an inability to initiate ESX-5 secretion would be predicted to negatively impact bacterial survival. We propose that *M. tuberculosis* encounters environments with reduced P_i availability during infection, which triggers the bacterium to secrete factors important for survival of these conditions through ESX-5. It is possible that ESX-5 is directly involved in P_i scavenging, similar to the proposed iron and/or zinc scavenging function of ESX-3 (Siegrist *et al.*, 2009, Serafini *et al.*, 2009). Alternatively, P_i limitation may simply be a signal to *M. tuberculosis* that it is within a nutrient-limited phagosomal environment and must activate ESX-5 and EsxB secretion to manipulate

phagosome function. Our future work will further investigate the relationship between P_i starvation and ESX-5 function and the importance of ESX-5 regulation during infection.

Experimental Procedures

Bacterial strains and culture conditions

M. tuberculosis Erdman and the derivative Δ*pstA1*, Δ*regX3*, Δ*pstA1*Δ*regX3*, Δ*regX3* pND*regX3* and Δ*pstA1*Δ*regX3* pND*regX3* mutant strains were constructed as previously described (Tischler *et al.*, 2013). The Δ*pstA1*Δ*ppe27-pe19*, Δ*pstA1*Δ*ppe27*, and Δ*pstA1*Δ*pe19* mutant strains were constructed as described (Ramakrishnan *et al.*, 2016). Bacterial cultures were grown at 37°C with aeration in Middlebrook 7H9 liquid medium (Difco) supplemented with albumin-dextrose-saline (ADS), 0.5% glycerol and 0.1% Tween-80, unless otherwise noted. Sauton's medium (3.67 mM KH_2PO_4, 2 mM $MgSO_4$-$7H_2O$, 9.5 mM citric acid, 0.19 mM ammonium iron (III) citrate, 26.64 mM L-asparagine, 6% glycerol, 0.01% $ZnSO_4$, pH 7.4) was used to grow cultures for protein isolation. P_i-free Sauton's medium contains all components of Sauton's complete medium except KH_2PO_4, and is buffered using 50 mM MOPS, pH 7.4. P_i-free 7H9 medium, used to culture bacteria used for RNA isolation during P_i-starvation, was prepared as previously described (Tischler *et al.*, 2013). Frozen stocks were prepared by growing liquid cultures to mid-exponential phase (OD_{600} 0.8-1.0) in complete 7H9 medium, then adding glycerol to 15% final concentration, and storing 1 ml aliquots at −80°C.

Quantitative RT-PCR

To test gene expression in P_i-rich growth conditions, *M. tuberculosis* bacteria were cultured in complete Middlebrook 7H9 medium to mid-exponential phase (OD_{600} 0.4-0.6). To assess induction of gene expression in response to P_i starvation, cultures were grown in 7H9 to mid-exponential phase (OD_{600} 0.4-0.6), then washed twice and resuspended at OD_{600} 0.2 in P_i-free 7H9. P_i-limited cultures were grown at 37°C with aeration and bacteria were collected at 0, 24, 48, 72 and 96 hours. Bacteria were collected by centrifugation (3700 x *g*, 10 min, 4°C). Total RNA was extracted using TRIzol (Invitrogen, CA) with 0.1% polyacryl carrier (Molecular Research Center, Inc) by bead beating with 0.1 mm zirconia beads (BioSpec Products). Equivalent amounts of total RNA were DNase-treated using Turbo DNase (Invitrogen) according to the manufacturer's instructions. Equivalent amounts of total RNA (500 ng) were converted to cDNA using the Transcriptor First Strand cDNA Synthesis Kit (Roche) and random hexamer primers. A no reverse transcriptase control was done for each RNA sample to quantify potential DNA contamination. The reverse transcription cycle parameters were as follows: 10 min at 25°C (annealing of primers), 60 min at 50°C (elongation), and 5 min at 85°C (heat inactivation of reverse transcriptase). Resulting cDNA was stored at −20°C until used for quantitative RT-PCR reactions.

Quantitative PCR primers to amplify an internal region of the genes or intergenic regions of interest (esxM, esxN, $espG_5$, $mycP_5$, $eccD_5$, ppe41, $eccB_5$, modD, espA, esxB, sigA, 16S rRNA, *pe19,* and the *ppe27-pe19* intergenic region) were designed with similar annealing temperatures (58-60°C) using either Primer Express software (Applied Biosystems) or ProbeFinder Assay Design software (Roche). Sequences of primers used are listed in

Supplementary Table 1. Quantitative RT-PCR reactions were prepared using 2x SYBR Green master mix (Roche), 2.5 μM primer mix and 1 μl cDNA. All reactions were run on a LightCycler 480 (Roche) using the following cycle parameters: 95°C for 10 min; 45 cycles of 95°C for 10s, 60°C for 20s, and 72°C for 20s with data collected once per cycle during the extension phase; and one cycle of 95°C for 5s, 65°C for 1m, 97°C with a ramp rate of 0.11 °C/s for generation of melting curves. Cycle threshold values (C_p,Roche nomenclature) were converted to copy numbers using standard curves for each gene, and gene copy numbers were normalized to *sigA* (P_i-rich cultures) or 16S rRNA (P_i-limited cultures).

Protein preparation for immunoblots

M. tuberculosis cultures were grown from frozen stocks to mid-exponential phase (OD_{600} 0.4-0.6) in complete Middlebrook 7H9. Bacteria were collected by centrifugation (2800 x *g*, 10 min), resuspended in 7H9 medium at a starting OD_{600} of 0.05-0.1 and grown to mid-exponential phase again. For experiments performed in P_i-rich conditions, bacteria were collected by centrifugation (2800 x *g*, 10 min) and used to inoculate Sauton's medium supplemented with 0.1% Tween-80 at a starting OD_{600} of 0.05-0.1. Cultures were incubated at 37°C with aeration to late exponential phase (OD_{600} 0.8-1.0), bacteria were collected by centrifugation (2800 x *g*, 10 min) and resuspended in Sauton's medium without Tween-80 at a starting OD_{600} of 0.8-1.0. Cultures were incubated at 37°C with aeration for 5 days before protein isolation. For P_i limitation experiments, the bacteria grown in 7H9 as above were collected by centrifugation (2800 x *g*, 10 min) and washed once with P_i-free Sauton's medium. Bacteria were then collected by centrifugation and resuspended in either Sauton's complete medium supplemented with Tween-80 (control) or P_i-free Sauton's medium supplemented with Tween-80 to which 250 μM KH_2PO_4 was added exogenously. Cultures were incubated at 37°C with aeration to late exponential phase (OD_{600} 0.8-1.0). Bacteria were collected by centrifugation (2800 x *g*, 10 min) and resuspended in the final medium used for protein secretion. For experiments conducted in P_i-replete conditions, Sauton's complete medium without Tween-80 was used. For P_i-limitation or P_i-titration samples, P_i-free Sauton's medium without Tween-80 to which 250, 25 or 2.5 μM KH_2PO_4 was added exogenously was used. For experiments to test whether P_i or K^+ was the relevant limiting ion, P_i-free Sauton's medium supplemented with 2.5 μM NaH_2PO_4 and 4 mM KCl (P_i limited) or 2.5 μM KCl and 4 mM NaH_2PO_4 (K^+ limited) was used. Cultures were incubated at 37°C with aeration for 5 days before protein was isolated.

Bacteria were collected by centrifugation (4700 x *g*, 15 min, 4°C). Culture supernatants were sterilized using 0.45 μm and then 0.22 μm syringe filters (Millipore). Complete EDTA-free protease inhibitor tablets (Roche) were added to each supernatant. Supernatants were concentrated roughly 25-fold by centrifugation (2400 x *g*, 4°C) using VivaSpin 5 kDa molecular weight cut-off spin columns (Sartorius). Whole cell lysates were prepared by washing the pellet twice in cold PBS, then resuspending in PBS containing Complete EDTA-free protease inhibitors (Roche) and bead beating with 0.1 mm zirconia beads (BioSpec Products). Beads and unlysed material were removed by centrifugation (600 x *g*, 5 min, 4°C). Large cell debris was removed from the lysate by centrifugation (3000 x *g*, 10 min, 4°C). Cell lysates were passaged through a Nanosep MF column with a 0.22 μm filter (Pall Life Sciences) by centrifugation (14000 x *g*, 3 min, 4°C) to remove any remaining

intact cells. Total protein concentration in each sample was quantified using the Pierce BCA Protein Concentration Assay kit (Thermo Scientific). Proteins were stored at 4°C for immediate use, or at −80°C with glycerol at 15% final concentration.

Immunoblot analysis

The indicated amounts of culture supernatant or whole cell lysate proteins were separated by sodium dodecyl sulfate polyacrylamide gel electrophoresis (SDS-PAGE) on Mini-PROTEAN TGX Any kD gels (Bio-Rad). Proteins were transferred to nitrocellulose membranes (Whatman) by electrophoresis and blocked overnight at 4°C in PBS-T (137 mM NaCl, 2.7 mM KCl, 10 mM Na_2HPO_4, 2 mM KH_2PO_4, 0.05% Tween-20) containing 5% non-fat milk powder. Membranes were washed in PBS-T and probed for 1 hour at room temperature with the primary antisera diluted in PBS-T containing 2.5% non-fat milk powder. Primary antisera were used at the following dilutions: rabbit α-EsxN 1:1000; rabbit α-$EspG_5$ 1:1000; rabbit α-$EccB_5$ 1:5000; rabbit α-PPE41 1:1000; rabbit α-EsxB 1:10,000; rat α-EspB 1:2000; rabbit α-ModD 1:5000; mouse α-GroEL2 1:10,000; rabbit α-Antigen 85 complex 1:5000. Membranes were washed in PBS-T again, and incubated for 1 hour at room temperature with the appropriate secondary antibody (either goat-anti-rabbit, rabbit-anti-mouse, or rabbit-anti-rat conjugated to HRP, Sigma) diluted 1:20,000 in PBS-T containing 2.5% non-fat milk powder. Membranes were washed again in PBS-T and the reactive bands were detected using SuperSignal West Pico substrate (Thermo Scientific) or Chemiluminescent Peroxidase Substrate (Sigma). Blots were exposed to film (Blue lite autorad film, GeneMate) and developed using a film processor (Konica, SRX-101A). Protein bands from scanned Western blot images were quantified using Image Studio Lite software, version 5.0. Images were imported as jpegs, and rectangular work areas of equivalent size without background correction were used to define regions for quantification of signal intensity.

Standard RT-PCR

To determine the length of transcripts initiating 5’ of *pe19*, *M. tuberculosis* bacteria were grown to mid-exponential phase (OD_{600} 0.4-0.6) in complete 7H9 (P_i-rich conditions) or grown to mid-exponential phase in complete 7H9, then washed twice, resuspended at OD_{600} 0.2 in P_i-free 7H9 and cultured for 24 hours (P_i-limiting conditions). RNA was extracted, treated with DNase, and converted to cDNA as described above. Standard PCR reactions were run using 1 μl of cDNA as template, 0.4 μM primers, and Recombinant Taq polymerse (Invitrogen). Cycle parameters were: 95°C 5 min; 40 cycles of 95°C 15 sec, 56°C 15 sec, 72°C 2.5 min; 72°C 10 min. The following primer pairs were used: ig4F/esxNR3, ig4F/espG5R1, ig3F/esxNR3 (Supplemental Table 1). PCR products were analyzed by gel electrophoresis.

Cloning and purification of His_6-RegX3

His_6-RegX3 was cloned in pET28b+, which contains a 6-histidine (His_6) tag and a kanamycin resistance cassette for selection. The *regX3* coding sequence was PCR amplified using *M. tuberculosis* Erdman genomic DNA as template (F primer: 5’-tt**catatg**atgaccagtgtgttgattgtggagga-3’, *Nde*I restriction site in bold; R primer: 5’-

tt**gctagc**ctagccctcgagtttgtagccca-3', *Nhe*I restriction site in bold), cloned in pCR2.1 (Invitrogen) and sequenced. *regX3* was removed from pCR2.1 by restriction with *Nde*I and *Nhe*I, gel purified, and ligated to similarly digested pET28b+. Recombinant N-terminal tagged His_6-RegX3 was expressed in *E. coli* BL21 (DE3). Bacteria were grown at 37°C with shaking to mid-exponential phase (OD_{600} 0.5) in LB containing 30 μg/ml kanamycin. His_6-RegX3 expression was induced with 0.1 mM IPTG for 3 hours at 37°C with shaking. Cells were concentrated 100-fold in lysis buffer (50 mM NaH_2PO_4, 300 mM NaCl, 10 mM imidazole, pH 8.0), incubated with 1 mg/ml lysozyme (30 min on ice) and lysed by sonication. His_6-RegX3 was bound to Ni-NTA agarose (Qiagen) for 1 hour at 4°C and loaded on a column. The column was washed with lysis buffer containing 20 mM imidazole. His_6-RegX3 was eluted using lysis buffer containing 250 mM imidazole. To remove contaminants that co-purified with His_6-RegX3, the protein was passed through an Amicon Ultra centrifugal filter with a 50 kDa cutoff (Millipore). Purified His_6-RegX3 was dialyzed in PBS and concentrated with Amicon Ultra centrifugal filters with a 10 kDa cutoff (Millipore).

Electrophoretic mobility shift assays (EMSAs)

Double-stranded DNA probes were PCR amplified using *M. tuberculosis* Erdman genomic DNA as template and appropriate primers (Supplementary Table 1). Probes were labeled using the DIG Gel Shift Kit, 2nd Generation (Roche), following the recommended protocols. Approximately 0.5 ng of DIG-labeled probe was added to binding reactions containing binding buffer (Roche), poly[d(I-C)], poly L-lysine, and 0.25 – 1 μg purified His_6-RegX3 in 20 ul total volume and incubated at room temperature for 15 min. Where appropriate, a 400-fold excess of unlabeled specific (Probe A) or non-specific (*dnaN*) competitor or anti-His_6 antibodies (THE™ His tag antibody, Genscript) were added to the reaction mixture. Binding reactions that include unlabeled competitor probe were incubated for 15 min at room temperature before adding the DIG-labeled probe, then incubated an additional 15 min. DNA-protein complexes were resolved using 5% native polyacrylamide gels, transferred and UV-crosslinked to nylon membranes (Roche). Membranes were washed with wash buffer (DIG wash and block buffer set, Roche), blocked for 30 min in blocking solution (Roche) and incubated with anti-DIG-AP antibodies (Roche) at a 1:10,000 dilution for 30 min at room temperature. Labeled probes were detected using CDP-Star ready-to-use substrate (Roche). Membranes were exposed to film (Blue lite autrorad film, Genemate) and developed using a film processor (Konica, SRX-101A).

Statistical Analysis

Student's unpaired t-test was used to compare wild-type *M. tuberculosis* to mutant strains. *P* values were calculated using GraphPad Prism 6 software. *P* values <0.05 were considered significant.

Supplementary Material

Refer to Web version on PubMed Central for supplementary material.

Acknowledgements

We thank Dr. Wilbert Bitter for generously providing anti-sera against the $EccB_5$, $EspG_5$, EsxN, and PPE41 proteins, Dr. Stewart Cole for providing anti-sera against EspB, and Dr. Jennifer L. Dale for critical reading of the manuscript. The following reagents were obtained through BEI Resources, NIAID, NIH: Polyclonal Anti-*Mycobacterium tuberculosis* CFP10 (Gene Rv3874, EsxB) (antiserum, Rabbit), NR-13801; Monoclonal Anti-*Mycobacterium tuberculosis* GroEL2 (Gene Rv0440), Clone IT-70 (DCA4) (produced *in vitro*), NR-13657; Polyclonal Anti-*Mycobacterium tuberculosis* Mpt32 (Gene Rv1860) (antiserum, Rabbit), NR-13807; and Polyclonal Anti-*Mycobacterium tuberculosis* Antigen 85 complex (FbpA/FbpB/FbpC; Genes Rv3804c, Rv1886c, Rv0129c) (antiserum, Rabbit), NR-13800. This work was supported by institutional startup funds from the University of Minnesota, and New Faculty and Equipment Grants from the University of Minnesota Foundation (A.D.T.).

References

Abdallah AM, Bestebroer J, Savage NDL, de Punder K, van Zon M, Wilson L, Korbee CJ, van der Sar AM, Ottenhoff THM, van der Wel NN, Bitter W, Peters PJ. Mycobacterial secretion systems ESX-1 and ESX-5 play distinct roles in host cell death and inflammasome activation. J. Immunol. 2011; 187:4744–4753. [PubMed: 21957139]

Bottai D, Di Luca M, Majlessi L, Frigui W, Simeone R, Sayes F, Bitter W, Brennan MJ, Leclerc C, Batoni G, Campa M, Brosch R, Esin S. Disruption of the ESX-5 system of *Mycobacterium tuberculosis* causes loss of PPE protein secretion, reduction of cell wall integrity and strong attenuation. Mol. Microbiol. 2012; 83:1195–1209. [PubMed: 22340629]

Chen JM, Zhang M, Rybniker J, Boy-Röttger S, Dhar N, Pojer F, Cole ST. *Mycobacterium tuberculosis* EspB binds phospholipids and mediates EsxA-independent virulence. Mol. Microbiol. 2013; 89:1154–1166. [PubMed: 23869560]

Cole ST, Brosch R, Parkhill J, Garnier T, Churcher C, Harris D, Gordon SV, Eiglmeier K, Gas S, Barry CEI, Takala F, Badcock K, Basham D, Brown D, Chillingworth T, Connor R, Davies R, Devlin K, Feltwell T, Gentles S, Hamlin N, Holroyd S, Hornsby T, Jagels K, Krogh A, McLean J, Moule S, Murphy L, Oliver K, Osborne J, Quail MA, Rajandream MA, Rogers J, Rutter S, Seeger K, Skelton J, Squares R, Squares S, Sulston JE, Taylor K, Whitehead S, Barrell BG. Deciphering the biology of Mycobacterium tuberculosis from the complete genome sequence. Nature. 1998; 393:537–544. [PubMed: 9634230]

Cortes T, Schubert OT, Rose G, Arnvig KB, Comas I, Aebersold R, Young DB. Genome-wide mapping of transcriptional start sites defines an extensive leaderless transcriptome in *Mycobacterium tuberculosis*. Cell Rep. 2013; 5:1121–1131. [PubMed: 24268774]

Daleke MH, van der Woude AD, Parret AHA, Ummels R, de Groot AM, Watson D, Piersma SR, Jiménez CR, Luirink J, Bitter W, Houben ENG. Specific chaperones for the type VII protein secretion pathway. J. Biol. Chem. 2012; 287:31939–31947. [PubMed: 22843727]

de Jonge MI, Pehau-Arnaudet G, Fretz MM, Romain F, Bottai D, Brodin P, Honoré N, Marchal G, Jiskoot W, England P, Cole ST, Brosch R. ESAT-6 from *Mycobacterium tuberculosis* dissociates from its putative chaperone CFP-10 under acidic conditions and exhibits membrane-lysing activity. J. Bacteriol. 2007; 189:6028–6034. [PubMed: 17557817]

Dobos KM, Swiderek K, Khoo KH, Brennan PJ, Belisle JT. Evidence for glycosylation sites on the 45-kilodalton glycoprotein of *Mycobacterium tuberculosis*. Infect. Immun. 1995; 63:2846–2853. [PubMed: 7622204]

Ekiert DC, Cox JS. Structure of a PE-PPE-EspG complex from *Mycobacterium tuberculosis* reveals molecular specificity of ESX protein secretion. Proc. Natl. Acad. Sci. USA. 2014; 111:14758–14763. [PubMed: 25275011]

Epstein W. The roles and regulation of potassium in bacteria. Prog. Nucleic Acid Res. Mol. Biol. 2003; 75:293–320. [PubMed: 14604015]

Fortune SM, Jaeger A, Sarracino DA, Chase MR, Sassetti CM, Sherman DR, Bloom BR, Rubin EJ. Mutually dependent secretion of proteins required for mycobacterial virulence. Proc. Natl. Acad. Sci. USA. 2005; 102:10676–10681. [PubMed: 16030141]

Gey van Pittius NC, Gamieldien J, Hide W, Brown GD, Siezen RJ, Beyers AD. The ESAT-6 gene cluster of *Mycobacterium tuberculosis* and other high G+C gram-positive bacteria. Genome Biol. 2001; 2:0044.0041–0044.0018.

Gonzalo-Asenio J, Mostowy S, Harders-Westerveen J, Huygen K, Hernandez- Pando R, Thole J, Behr M, Gicquel B, Martin C. PhoP: a missing piece in the intricate puzzle of *Mycobacterium tuberculosis* virulence. PLoS One. 2008; 3:e3496. [PubMed: 18946503]

Guinn KM, Hickey MJ, Mathur SK, Zakel KL, Grotzke JE, Lewinsohn DM, Smith S, Sherman DR. Individual RD1-region genes are required for export of ESAT-6/CFP-10 and for virulence of *Mycobacterium tuberculosis*. Mol. Microbiol. 2004; 51:359–370. [PubMed: 14756778]

Himpens S, Locht C, Supply P. Molecular characterization of the mycobacterial SenX3-RegX3 two-component system: evidence for autoregulation. Microbiol. 2000; 146:3091–3098.

Houben D, Demangel C, van Ingen J, Perez J, Baldeon L, Abdallah AM, Caleechurn L, Bottai D, van Zon M, de Punder K, van der Laan T, Kant A, Bossers-de Vries R, Willemsen P, Bitter W, van Soolingen D, Brosch R, van der Wel N, Peters PJ. ESX-1-mediated translocation to the cytosol controls virulence of mycobacteria. Cell Microbiol. 2012a; 14:1287–1298. [PubMed: 22524898]

Houben ENG, Bestebroer J, Ummels R, Wilson L, Piersma SR, Jiménez CR, Ottenhoff THM, Luirink J, Bitter W. Composition of the type VII secretion system membrane complex. Mol. Microbiol. 2012b; 86:472–484. [PubMed: 22925462]

Houben ENG, Korotkov KV, Bitter W. Take five - Type VII secretion systems of *Mycobacteria*. Biochim. Biophys. Acta. 2014; 1843:1707–1716. [PubMed: 24263244]

Hsu T, Hingley-Wilson SM, Chen B, Chen M, Dai AZ, Morin PM, Marks CB, Padiyar J, Goulding C, Gingery M, Eisenberg D, Russell DG, Derrick SC, Collins FM, Morris SL, King CH, Jacobs WR Jr. The primary mechanism of attenuation of bacillus Calmette-Guerin is a loss of secreted lytic function required for invasion of lung interstitial tissue. Proc. Natl. Acad. Sci. USA. 2003; 100:12420–12425. [PubMed: 14557547]

Kennedy GM, Hooley GC, Champion MM, Medie FM, Champion PAD. A novel ESX-1 locus reveals that surface-associated ESX-1 substrates mediate virulence in *Mycobacterium marinum*. J. Bacteriol. 2014; 196:1877–1888. [PubMed: 24610712]

Korotkova N, Freire D, Phan TH, Ummels R, Creekmore CC, Evans TJ, Wilmanns M, Bitter W, Parret AHA, Houben ENG, Korotkov KV. Structure of the *Mycobacterium tuberculosis* type VII secretion system chaperone EspG5 in complex with PE25-PPE41 dimer. Mol. Microbiol. 2014; 94:367–382. [PubMed: 25155747]

Lamarche MG, Wanner BL, Crépin S, Harel J. The phosphate regulon and bacterial virulence: a regulatory network connecting phosphate homeostasis and pathogenesis. FEMS Microbiol. Rev. 2008; 32:461–473. [PubMed: 18248418]

Ligon LS, Hayden JD, Braunstein M. The ins and outs of *Mycobacterium tuberculosis* protein export. Tuberculosis (Edinb). 2012; 92:121–132. [PubMed: 22192870]

Maciag A, Dainese E, Rodriguez GM, Milano A, Provvedi R, Pasca MR, Smith I, Palu G, Riccardi G, Manganelli R. Global analysis of the *Mycobacterium tuberculosis* Zur (FurB) regulon. J. Bacteriol. 2007; 189:730–740. [PubMed: 17098899]

Manzanillo PS, Shiloh MU, Portnoy DA, Cox JS. *Mycobacerium tuberculosis* activates the DNA-dependent cytosolic surveillance pathway within macrophages. Cell Host Microbe. 2012; 11:469–480. [PubMed: 22607800]

McLaughlin B, Chon JS, MacGurn JA, Carlsson F, Cheng TL, Cox JS, Brown EJ. A mycobacterium ESX-1-secreted virulence factor with unique requirements for export. PLoS Pathog. 2007; 3:e105. [PubMed: 17676952]

Pang X, Samten B, Cao G, Wang X, Tvinnereim AR, Chen X-L, Howard ST. MprAB regulates the *espA* operon in *Mycobacterium tuberculosis* and modulates ESX-1 function and host cytokine response. J. Bacteriol. 2013; 195:66–75. [PubMed: 23104803]

Parish T, Smith DA, Roberts G, Betts J, Stoker NG. The *senX3-regX3* two-component regulatory system of *Mycobacterium tuberculosis* is required for virulence. Microbiol. 2003; 149:1423–1435.

Peyron P, Vaubourgeix J, Poquet Y, Levillain F, Botanch C, Bardou F, Daffé M, Emile J-F, Marchou B, Cardona PJ, de Chastellier C, Altare F. Foamy macrophages from tuberculous patients' granulomas

constitute a nutrient-rich reservoir for *M. tuberculosis* persistence. PLoS Pathog. 2008; 4:e1000204. [PubMed: 19002241]

Raghavan S, Manzanillo P, Chan K, Dovey C, Cox JS. Secreted transcription factor controls *Mycobacterium tuberculosis* virulence. Nature. 2008; 454:717–721. [PubMed: 18685700]

Ramakrishnan P, Aagesen AM, McKinney JD, Tischler AD. *Mycobacterium tuberculosis* resists stress by regulating PE19 expression. Infect. Immun. 2016; 82 in press.

Rifat D, Bishai WR, Karakousis PC. Phosphate depletion: a novel trigger for *Mycobacterium tuberculosis* persistence. J. Infect. Dis. 2009; 200:1126–1135. [PubMed: 19686042]

Rodriguez GM, Voskuil MI, Gold B, Schoolnik GK, Smith I. *ideR*, an essential gene in *Mycobacterium tuberculosis*: role of IdeR in iron-dependent gene expression, iron metabolism, and oxidative stress response. Infect. Immun. 2002; 70:3371–3381. [PubMed: 12065475]

Russell DG, Cardona PJ, Kim MJ, Allain S, Altare F. Foamy macrophages and the progession of the human tuberculosis granuloma. Nat. Immunol. 2009; 10:943–948. [PubMed: 19692995]

Russell DG, VanderVen BC, Abramovitch RB, Kim MJ, Homolka S, Niemann S, Rohde KH. *Mycobacterium tuberculosis* wears what it eats. Cell Host Microbe. 2010; 8:68–76. [PubMed: 20638643]

Sampson SL. Mycobacterial PE/PPE proteins at the host-pathogen interface. Clin. Dev. Immunol. 2011; 2011:497203. [PubMed: 21318182]

Sayes F, Sun L, Di Luca M, Simeone R, Degaiffier N, Fiette L, Esin S, Brosch R, Bottai D, Leclerc C, Majlessi L. Strong immunogenicity and cross- reactivity of *Mycobacterium tuberculosis* ESX-5 type VII secretion-encoded PE PPE proteins predicts vaccine potential. Cell Host Microbe. 2012; 11:352–363. [PubMed: 22520463]

Serafini A, Boldrin F, Palu G, Manganelli R. Characterization of a *Mycobacterium tuberculosis* ESX-3 conditional mutant: essentiality and rescue by iron and zinc. J. Bacteriol. 2009; 191:6340–6344. [PubMed: 19684129]

Shell SS, Wang J, Lapierre P, Mir M, Chase MR, Pyle MM, Gawande R, Ahmad R, Sarracino DA, Ioerger TR, Fortune SM, Derbyshire KM, Wade JT, Gray TA. Leaderless transcripts and small proteins are common features of the mycobacterial translational landscape. PLoS Genet. 2015; 4:e1005641. [PubMed: 26536359]

Siegrist MS, Unnikrishnan M, McConnell MJ, Borowsky M, Cheng TY, Siddiqi N, Fortune SM, Moody DB, Rubin EJ. Mycobacterial ESX-3 is required for mycobactin-mediated iron acquisition. Proc. Natl. Acad. Sci. USA. 2009; 106:18792–18797. [PubMed: 19846780]

Stanley SA, Raghavan S, Hwang WW, Cox JS. Acute infection and macrophage subversion by *Mycobacterium tuberculosis* require a specialized secretion system. Proc. Natl. Acad. Sci. USA. 2003; 100:13001–13006. [PubMed: 14557536]

Stoop EJM, Bitter W, van der Sar AM. Tubercle bacilli rely on a type VII army for pathogenicity. Trends Microbiol. 2012; 20:477–484. [PubMed: 22858229]

Tischler AD, Leistikow RL, Kirksey MA, Voskuil MI, McKinney JD. *Mycobacterium tuberculosis* requires phosphate-responsive gene regulation to resist host immunity. Infect. Immun. 2013; 81:317–328. [PubMed: 23132496]

Wagner D, Maser J, Lai B, Cai Z, Barry CEI, Bentrup KHZ, Russell DG, Bermudez LE. Elemental analysis of *Mycobacterium avium-, Mycobacterium tuberculosis-*, and *Mycobacterium smegmatis*-containing phagosomes indicates pathogen-induced microenvironments within the host cell's endosomal system. J. Immunol. 2005; 174:1491–1500. [PubMed: 15661908]

Wagner D, Maser J, Moric I, Vogt S, Kern WV, Bermudez LE. Elemental analysis of the *Mycobacterium avium* phagosome in Balb/c mouse macrophages. Biochem. Biophys. Res. Commun. 2006; 344:1346–1351. [PubMed: 16650826]

Zhang M, Chen JM, Sala C, Rybniker J, Dhar N, Cole ST. EspI regulates the ESX-1 secretion system in response to ATP levels in *Mycobacterium tuberculosis*. Mol. Microbiol. 2014; 93:1057–1065. [PubMed: 25039394]

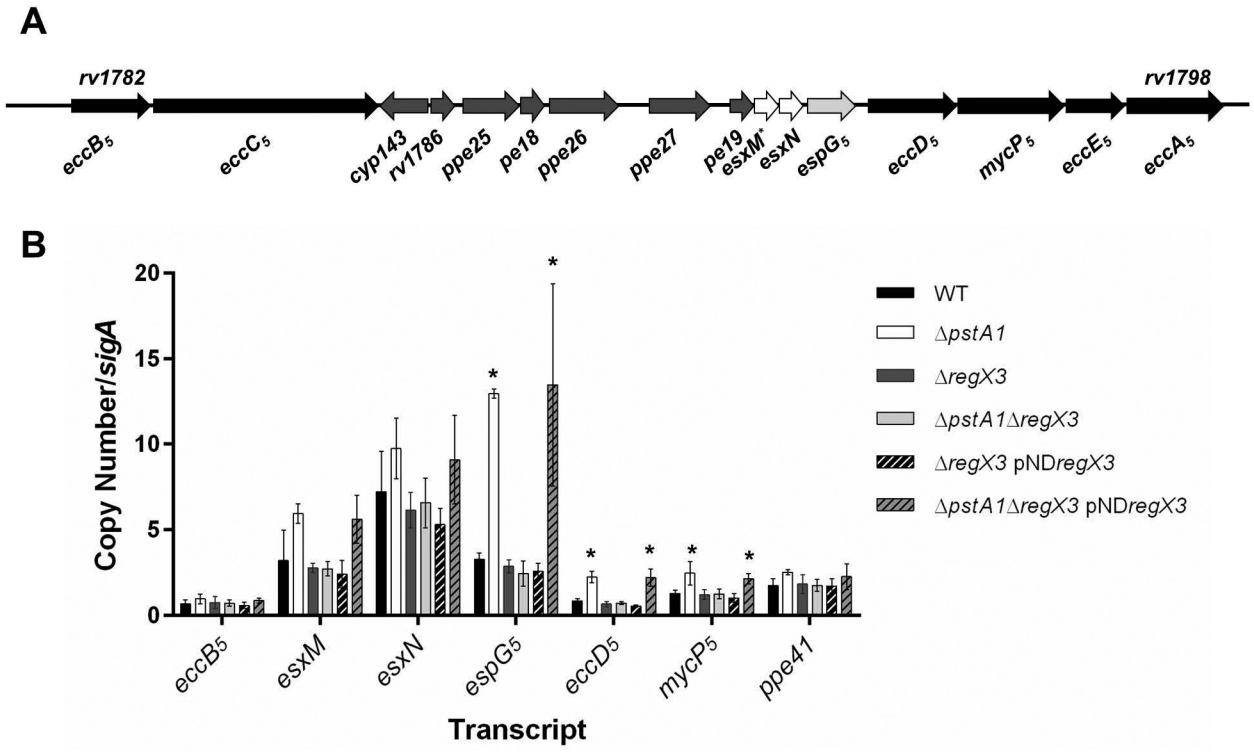

Figure 1.

Overexpression of *esx-5* genes in the Δ*pstA1* mutant is RegX3-dependent. A. Schematic representation of the *esx-5* locus. Genes encoding ESX-5 conserved components are in black, known ESX-5 substrates are in white, and a known ESX-5 cytoplasmic chaperone is in light gray. Genes with no confirmed function in ESX-5 secretion are in dark gray. The * indicates a gene with a known frame-shift mutation.

B. Quantitative RT-PCR analysis of *esx-5* transcription. Wild-type *M. tuberculosis* Erdman (WT), Δ*pstA1*, Δ*regX3*, Δ*pstA1*Δ*regX3*, Δ*regX3* pND*regX3* and Δ*pstA1*Δ*regX3* pND*regX3* were cultured in P_i-rich 7H9 medium to mid-exponential phase and RNA was extracted. Abundance of the *eccB*$_5$, *esxM, esxN, espG*$_5$, *eccD*$_5$, *mycP*$_5$ and *ppe41* transcripts relative to *sigA* was determined by quantitative RT-PCR. Data shown are the means +/- standard deviations of three independent experiments. Asterisks indicate a statistically significant difference in transcript abundance compared to the WT control ($P < 0.05$).

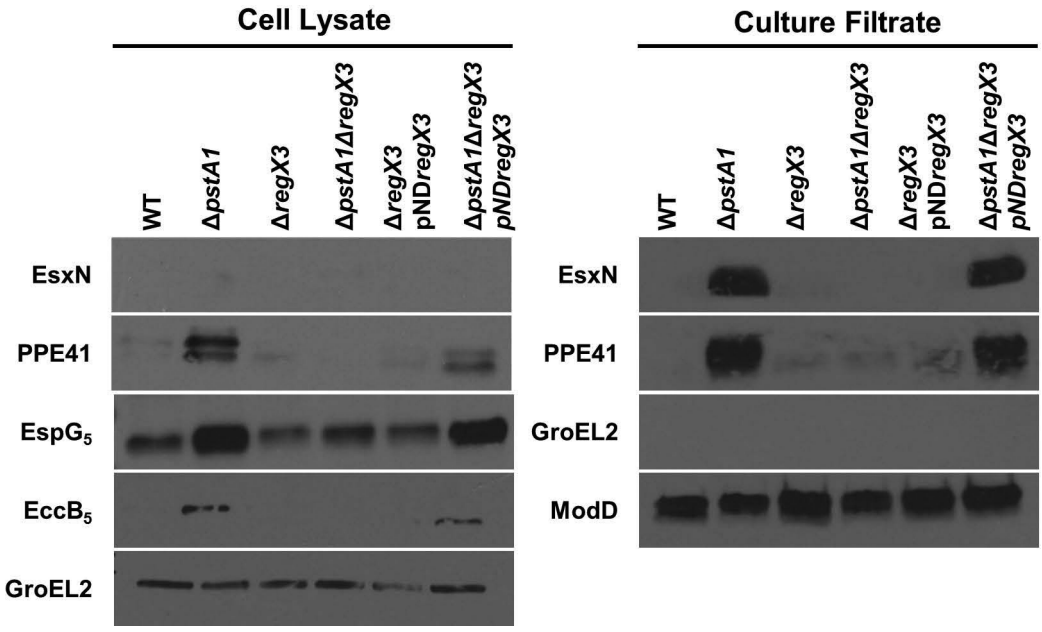

Figure 2.

Hyper-secretion of ESX-5 substrates by the Δ*pstA1* mutant requires RegX3. Wild-type *M. tuberculosis* Erdman (WT), Δ*pstA1*, Δ*regX3*, Δ*pstA1*Δ*regX3,* Δ*regX3* pND*regX3* and Δ*pstA1*Δ*regX3* pND*regX3* were cultured in Sauton's complete medium without Tween-80 for 5 days. 10 μg of cell lysate (CL) and 4 μg of culture filtrate (CF) proteins were subjected to SDS-PAGE and Western blot analysis. Antibodies used are indicated. Anti-GroEL2 was used as both a loading control for the CL fraction and a cell lysis control in the CF fraction. Anti-ModD was used as a loading control for the CF fraction. Results shown are from a single experiment and are representative of 3 independent experiments.

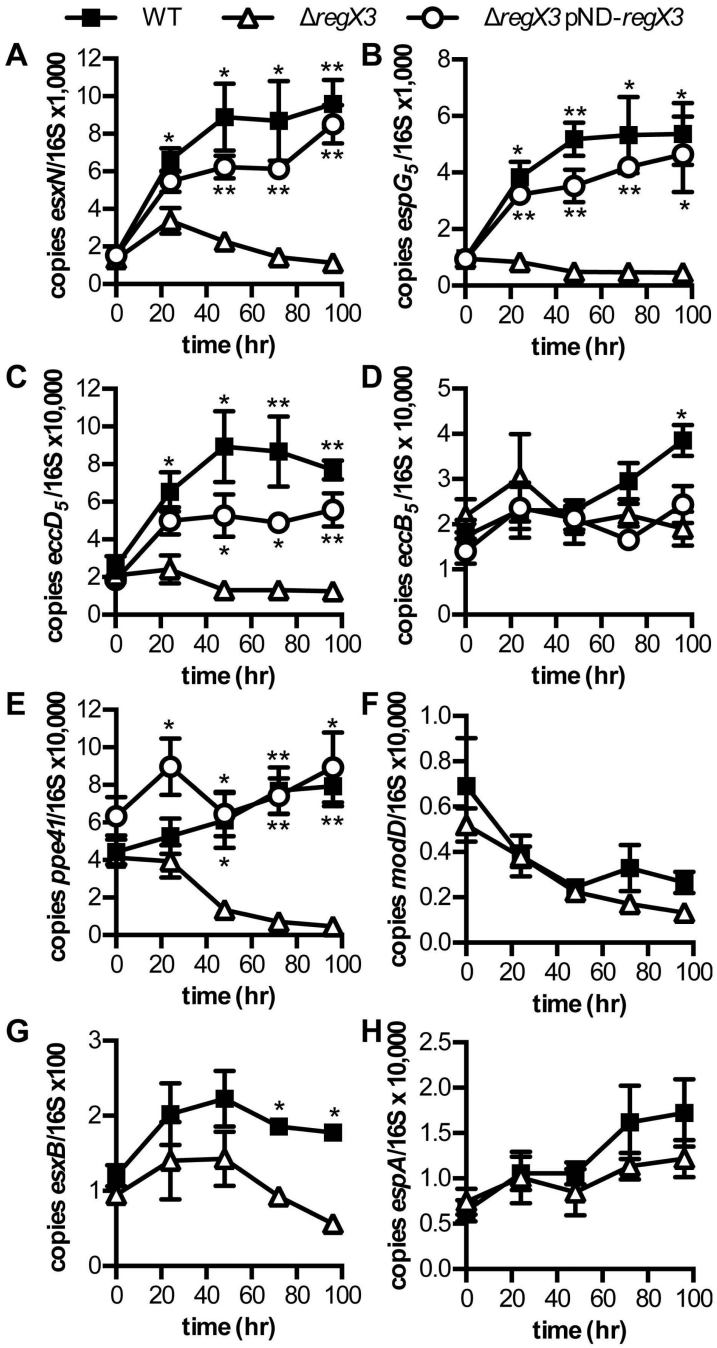

Figure 3.

Induction of ESX-5 genes by phosphate limitation requires RegX3. Wild-type *M. tuberculosis* Erdman (WT), Δ*regX3*, and Δ*regX3* pND*regX3* were cultured in P_i-free 7H9 medium for 96 hours. RNA was extracted at 0, 24, 48, 72 and 96 hours. Abundance of the *esxN, espG*$_5$, *eccD*$_5$, *eccB*$_5$, *ppe41*, *modD*, *esxB*, and *espA* transcripts relative to 16S rRNA was determined by quantitative RT-PCR. Data shown are the means +/− standard deviations of three independent experiments. Asterisks indicate statistically significant differences in

transcript abundance between WT and Δ*regX3* or Δ*regX3* pND*regX3* and Δ*regX3*: * $P < 0.05$; ** $P < 0.005$

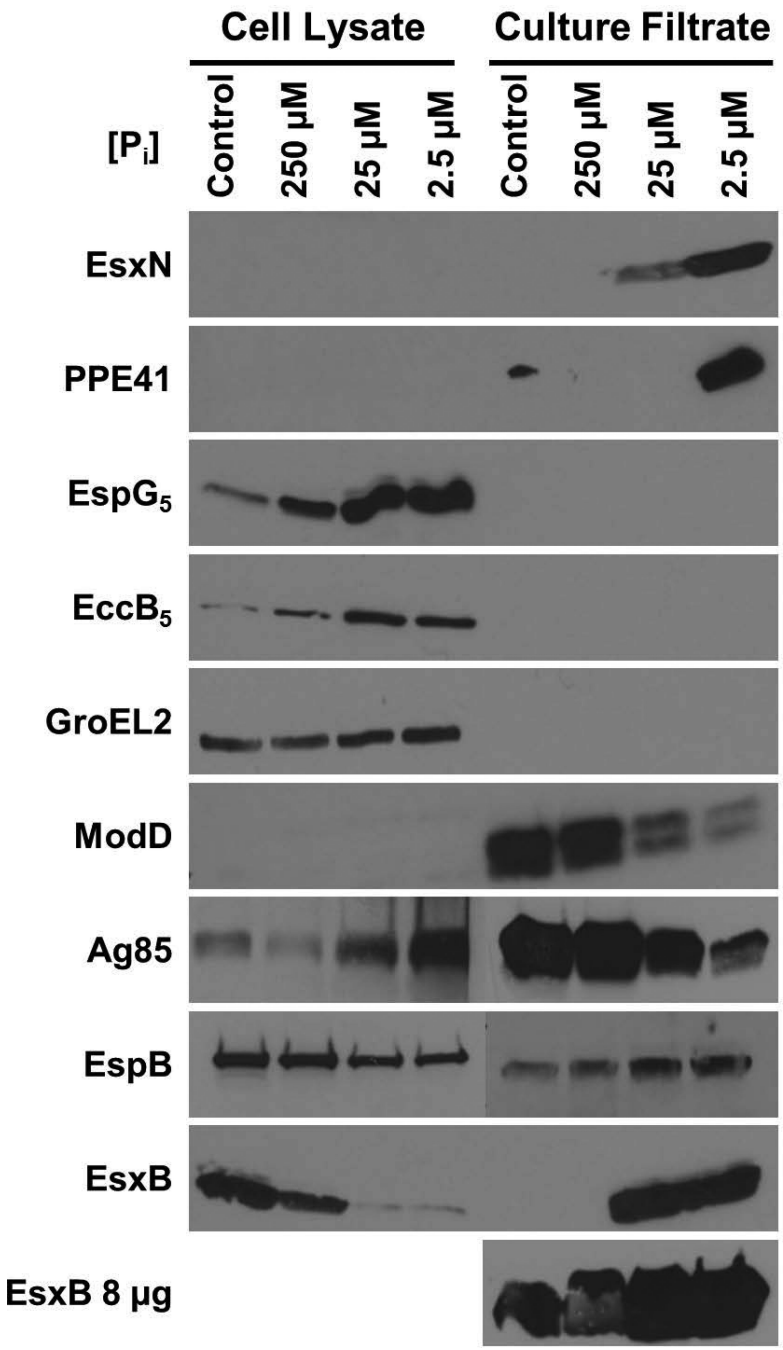

Figure 4.

Phosphate limitation induces ESX-5 and ESX-1 protein secretion.

Wild-type *M. tuberculosis* Erdman was grown for 5 days in Sauton's complete medium without Tween-80 (control) or P_i-free Sauton's medium without Tween-80 to which 250, 25, or 2.5 µM KH_2PO_4 was added exogenously. 10 µg of cell lysate (CL) and 4 µg or 8 µg (as indiciated) of culture filtrate (CF) proteins were subjected to SDS-PAGE and Western blot analysis. Antibodies used are indicated. Anti-GroEL2 was used as both a loading control for the CL fraction and a cell lysis control in the CF fraction. Anti-ModD was used as a loading

control for the CF fraction. Results shown are from a single experiment and are representative of 2 independent experiments.

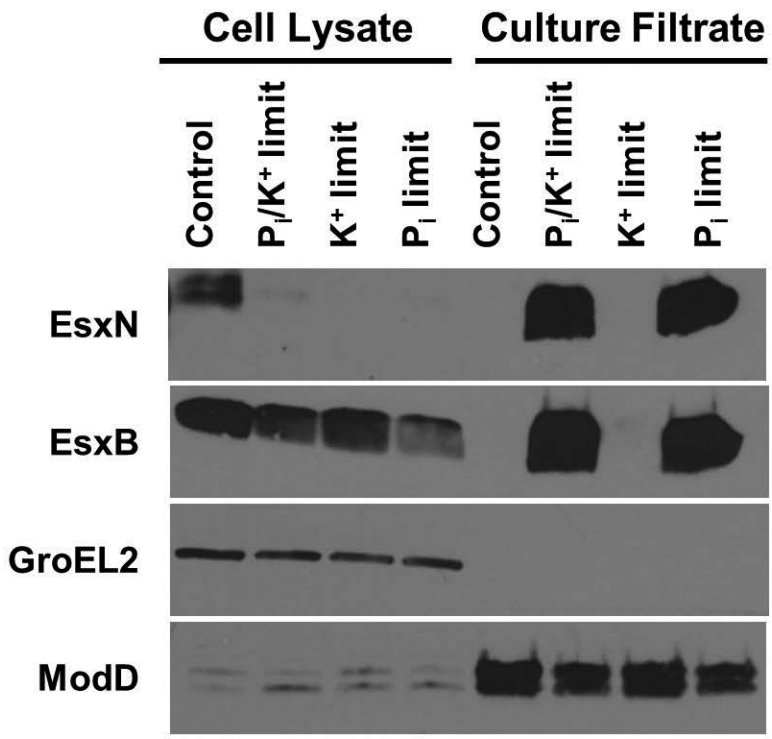

Figure 5.

Secretion of the ESX-1 substrate EsxB is induced by phosphate limitation. Wild-type *M. tuberculosis* Erdman was cultured for 5 days in Sauton's complete medium without Tween-80 (control), or P_i-free Sauton's medium without Tween-80 to which either 2.5 μM KH_2PO_4 (P_i and K^+ limitation), 2.5 μM NaH_2PO_4 and 4 mM KCl (P_i limitation) or 2.5 μM KCl and 4 mM NaH_2PO_4 (K^+ limitation) was added exogenously. 10 μg of cell lysate (CL) and 4 μg of culture filtrate (CF) proteins were subjected to SDS-PAGE and Western blot analysis. Anti-GroEL2 was used as both a loading control for the CL fraction and a cell lysis control in the CF fraction. Anti-ModD was used as a loading control for the CF fraction. Results shown are from a single experiment and are representative of 3 independent experiments.

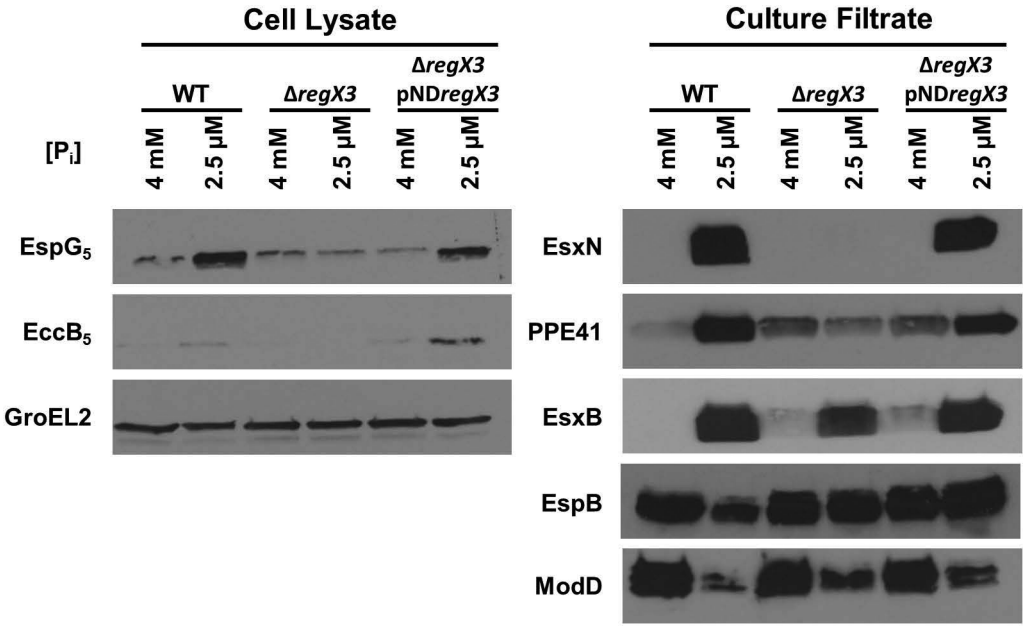

Figure 6.

RegX3 is required for induction of ESX-5 protein secretion in response to phosphate limitation.

Wild-type *M. tuberculosis* Erdman (WT), Δ*regX3*, and Δ*regX3* pND*regX3* strains were cultured for 5 days either in Sauton's complete medium without Tween-80 (control) or in P_i-free Sauton's medium without Tween-80 to which 2.5 μM KH_2PO_4 was added exogenously. 10 μg of cell lysate (CL) and 4 μg of culture filtrate (CF) proteins were subjected to SDS-PAGE and Western blot analysis. Anti-GroEL2 was used as both a loading control for the CL fraction and a cell lysis control in the CF fraction (data not shown). Anti-ModD was used as a loading control for the CF fraction. Results shown are representative of 3 independent experiments.

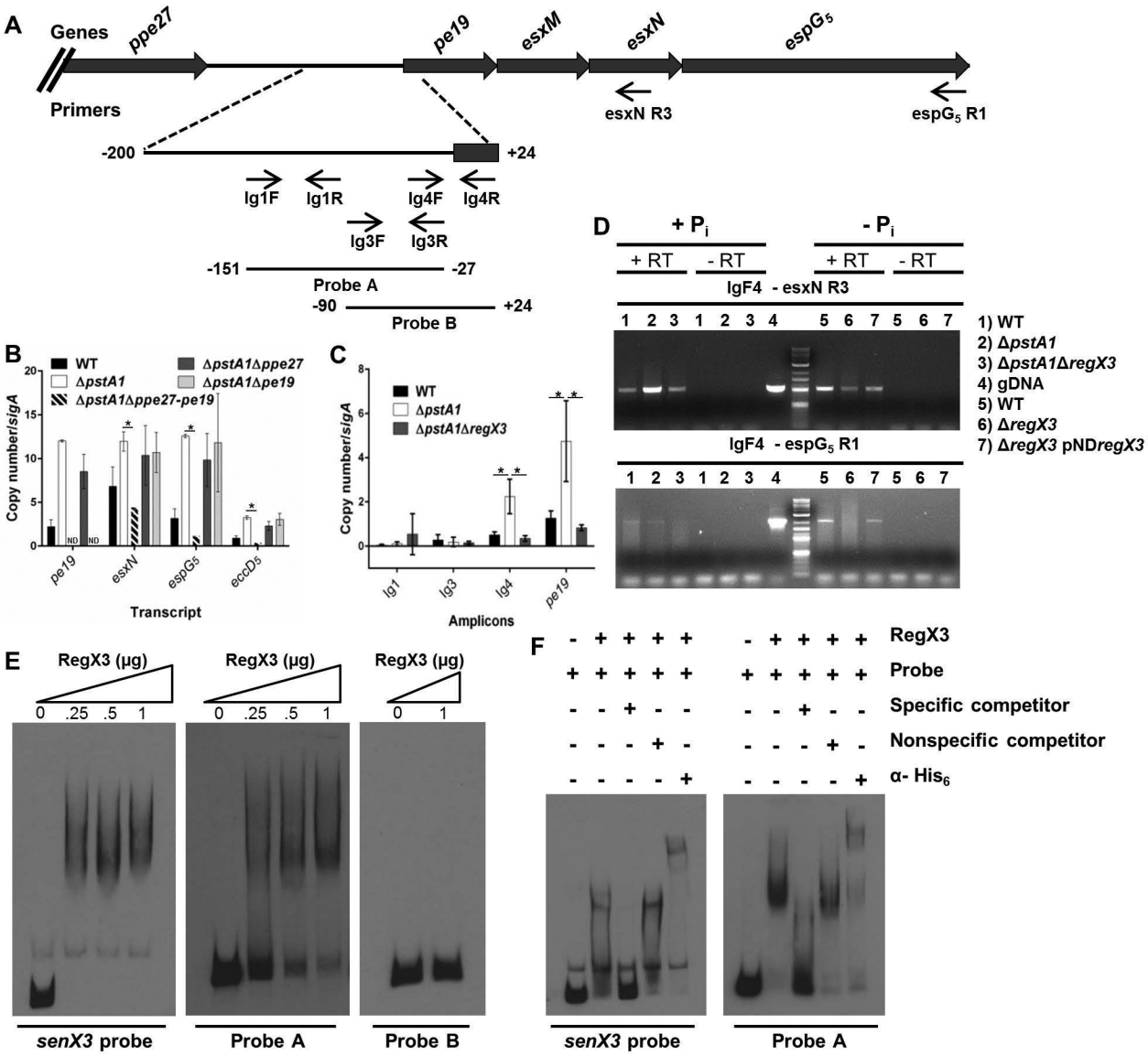

Figure 7.

Determining the RegX3 binding site within the *esx-5* locus.

A. Schematic representation of the 3' *esx-5* locus. The intergenic region between *ppe27* and *pe19* is enlarged. Locations of relevant primers and probes used for EMSAs are indicated.

B. Quantitative RT-PCR analysis of *esx-5* transcription. Wild-type *M. tuberculosis* Erdman (WT), Δ*pstA1*, Δ*pstA1*Δ*ppe27-pe19,* Δ*pstA1*Δ*ppe27* and Δ*pstA1*Δ*pe19* were cultured in P_i-rich 7H9 medium to mid-exponential phase and RNA was extracted. Abundance of the *pe19, esxN, espG*$_5$, and *eccD*$_5$ *transcripts* relative to *sigA* was determined by quantitative RT-PCR. Data shown are the means +/- standard deviations of three experiments. Asterisks indicate statistically significant differences in transcript abundance between Δ*pstA1* and Δ*pstA1*Δ*ppe27-pe19* ($P < 0.05$).

C. Quantitative RT-PCR analysis of mRNA levels of amplicons within the *ppe27-pe19* intergenic region and *pe19*. WT, Δ*pstA1* and Δ*pstA1*Δ*regX3* strains were cultured in P_i-rich 7H9 medium to mid-exponential phase and RNA was extracted. Abundance of the

amplicons relative to *sigA* was determined by quantitative RT-PCR. Data shown are the means +/− standard deviations of three independent experiments. Asterisks indicate statistically significant differences in amplicon abundance between Δ*pstA1* and either WT or Δ*pstA1*Δ*regX3* ($P < 0.05$).

D. Identification of an *esx-5* operon by RT-PCR. WT, Δ*pstA1,* and Δ*pstA1*Δ*regX3* were cultured in P_i-rich 7H9 medium to mid-exponential phase (+P_i). WT, Δ*regX3* and Δ*regX3* pND−*regX3* strains were cultured for 24 hours in 7H9 no P_i (−P_i). RNA was extracted, reverse transcribed to cDNA, and PCR amplified using the indicated primers. +RT and −RT denote cDNA synthesis reactions where reverse transcriptase was included or excluded, respectively. gDNA was included as a template for each primer pair as a positive control.

E. EMSA analysis of binding between purified His_6-RegX3 the SenX3 probe (positive control), and Probes A and B probes. 0.5 ng of DIG-labeled probe was incubated with increasing concentrations (0-1 μg) of purified recombinant His_6-RegX3.

F. EMSA analysis of RegX3 binding specificity. DIG-labeled *senX3* probe (positive control) or Probe A was incubated with purified recombinant His_6-RegX3. Unlabeled competitors (specific or non-specific) or α-His_6 antibodies were added to the binding reactions as indicated by the + symbols.

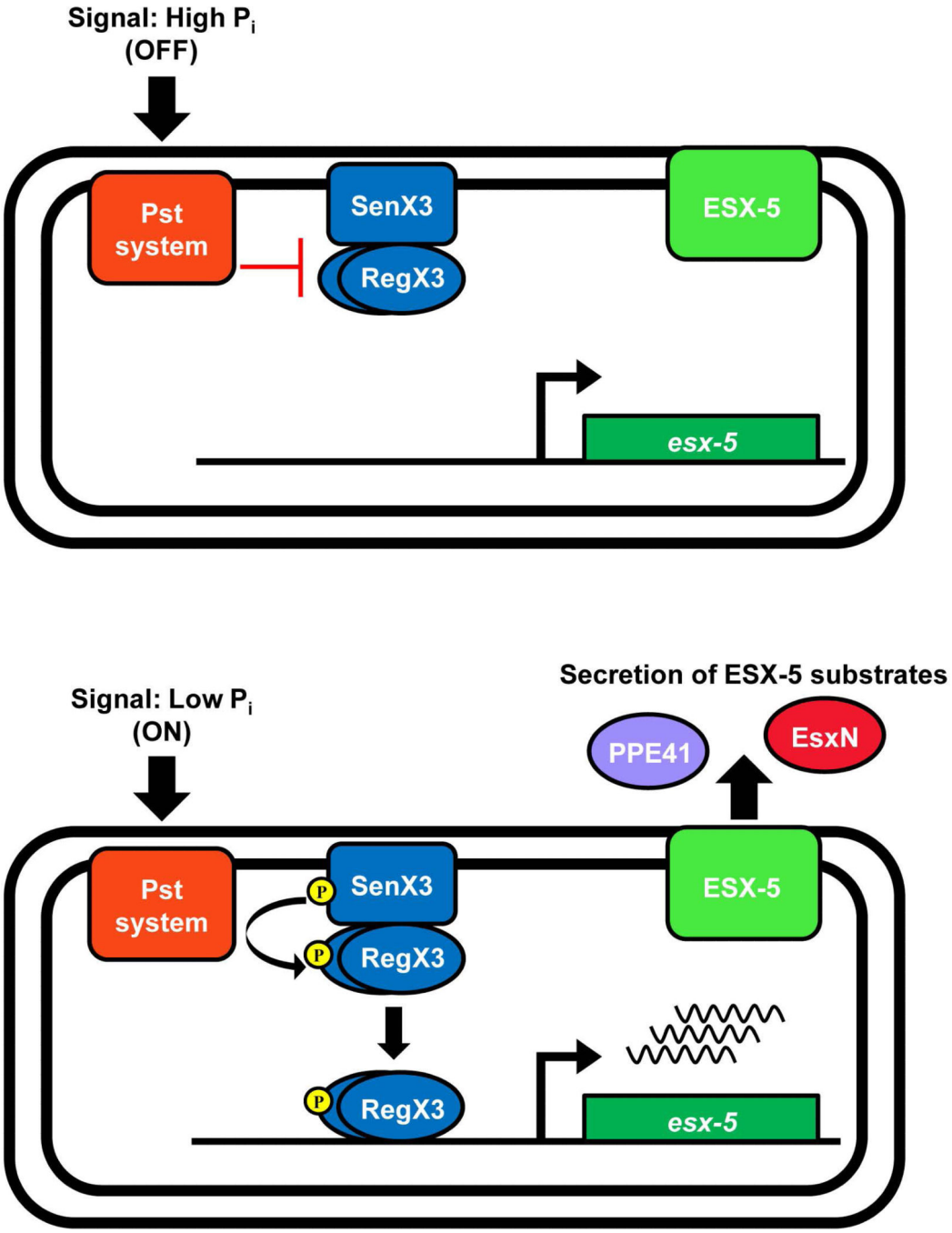

Figure 8.

Model of ESX-5 regulation by the Pst/SenX3-RegX3 system in response to phosphate availability. When the external P_i concentration is high, the Pst system inhibits the SenX3-RegX3 two-component system, *esx-5* genes are transcribed at a basal level, there is no induction of secretion and ESX-5 is 'off'. When external P_i is limiting, inhibition of SenX3-RegX3 by the Pst system is relieved, turning the ESX-5 system 'on'. SenX3 activates RegX3

via phospho-transfer, allowing RegX3 to bind a promoter within the *esx-5* locus to initiate transcription, leading to increased secretion of ESX-5 substrates.